Novel Mode Selection Schemes for Buffer-Aided Cooperative NOMA System

Peng Xu, *Member, IEEE*, Yunwu Wang, Gaojie Chen, *Senior Member, IEEE*, Ioannis Krikidis, *Fellow, IEEE* and Kai-Kit Wong, *Fellow, IEEE*

***Abstract*—This paper investigates a cooperative non-orthogonal multiple access (C-NOMA) system, where the NOMA and buffer-aided cooperative transmission modes between the users are integrated. Two novel mode selection schemes are proposed, which adaptively select the NOMA and cooperative modes according to different buffer states and communication environments. These two proposed schemes are termed single-core state (SCS) and dual-core state (DCS) schemes since they correspond to single and dual-core buffer states. These core states are carefully chosen, which ensure not only a sufficient amount of available transmission modes or links but also a small number of stored packets at each buffer. The closed-form expressions of the outage probabilities and average delays of the proposed schemes are derived and verified by simulation results. Asymptotic performance analysis is also performed, revealing that both proposed schemes achieve the full diversity within the minimum required buffer size of two. Analytical and simulation results show that the proposed SCS and DCS schemes ensure favourable outage performance and the lowest delay, respectively.**

***Index Terms*—Cooperative NOMA, buffer-aided, outage probability, diversity gain, average delay.**

I. Introduction

In recent years, non-orthogonal multiple access (NOMA) has been recognized as one of the most promising multiple access techniques for the next-generation of wireless communications due to its high spectral efficiency in comparison with conventional orthogonal multiple access (OMA) [1]–[5]. The main principle of NOMA is that multiple users can be served on the same orthogonal resource block. In particular, the transmitter uses superposition coding to serve more than one receiver in downlink power-domain NOMA systems, and the receivers employ successive interference cancellation (SIC) to decode their messages.

The combination of NOMA and cooperative techniques has attracted much attention recently. Cooperative NOMA (C-NOMA) mainly includes the types of dedicated-relay cooperation [6]–[11] and user-based cooperation [12]–[16]. The difference between them is that the relay nodes without information to receive or transmit are responsible for users' message transmission, while the cooperative user nodes need to receive their own messages and help other users for message transmission. Motivated by the benefits of these two cooperation schemes, the authors in [17] investigated a NOMA system with combined dedicated-relay and user-based cooperation, to improve the reliability of the system further.

The spectral efficiency of C-NOMA is often limited by half-duplex constraints at the cooperative nodes. To this end, the buffer-aided relaying technique, which has the ability to enhance the freedom of link selection [18]–[26], was applied to C-NOMA systems recently to enhance the transmission performance further. For buffer-aided C-NOMA systems, the critical challenge is to design an efficient link/mode selection scheme to integrate NOMA and buffer-aided cooperative transmission [27]–[33]. The authors in [27]–[29] investigated C-NOMA systems with a single buffer-aided relay, and the authors in [30]–[33] investigated C-NOMA systems with multiple buffer-aided relays. In addition, C-NOMA with bidirectional buffer-aided cooperative users was first introduced in our previous work [34], and the "priority to NOMA (P2N)" scheme was proposed, which combines the NOMA transmission and the conventional buffer state-based cooperative transmission in [19], to balance the tradeoff between the outage probability and the average delay.

Due to the existence of different types of transmission modes and a large amount of time-varying buffer states, the design of optimal buffer-aided schemes in C-NOMA systems with delay constraints is still an open issue. Take the P2N scheme in [34] for instance. It always allocates the priority to perform the t NOMA mode, which may impede the change of the unfavourable (e.g. full or empty) buffer states and harm the system performance. Moreover, the P2N scheme also employs the buffer-aided cooperative strategy in [19] to manage the buffer state evolution by making each buffer stay at the state with two stored packets, which results in a high average delay. To further enhance the transmission reliability and reduce the average delay of the C-NOMA systems, this paper further exploits the performance of the buffer-aided C-

The work of P. Xu and Y. Wang was supported in part by the National Natural Science Foundation of China under Grant 62001076 and 62071078, in part by Institute for Advanced Sciences, Chongqing University of Posts and Telecommunication (E011A2022324), and in part by the Postgraduate Student Research Innovation Project of Chongqing under Grant CYS21299. The work of Ioannis Krikidis has received funding from the European Research Council (ERC) under the European Union's Horizon 2020 research and innovation programme (Grant agreement No. 81981). The work of K. K. Wong is supported in part by the EPSRC under grant EP/T015985/1. (*Corresponding Author: Gaojie Chen.*)

P. Xu and Y. Wang are with the School of Communication and Information Engineering, Chongqing University of Posts and Telecommunications, Chongqing 400065, China and also with the Chongqing Key Laboratory of Mobile Communications Technology, Chongqing 400065, China (Email: xupeng@cqupt.edu.cn, wangyunw@163.com).

G. Chen is with 5GIC & 6GIC, Institute for Communication Systems, University of Surrey, Guildford, UK (Emails: gaojie.chen@surrey.ac.uk).

I. Krikidis is with Dept. of Electrical and Computer Engineering, University of Cyprus, Kallipoleos 75, Nicosia 1678, Cyprus. (Email: krikidis@ucy.ac.cy).

K. Wong is with the Department of Electronic and Electrical Engineering, University College London, London WC1E 7JE, U.K. (Email: kai-kit.wong@ucl.ac.uk).

NOMA system for downlink transmission, where an access point (AP) communicates with a pair of users at the aid of buffers, and the NOMA and bidirectional buffer-aided cooperative transmission modes between the users are integrated. The considered system model is appropriate for a various of applications where power-domain NOMA is used to serve two users at the same orthogonal frequency division multiple access (OFDMA) subcarrier. Meanwhile, it is beneficial to employ buffer-aided cooperation between the two users to enhance the outage performance, if a slight loss of the delay performance is allowed for the services.

In this paper, we propose two novel mode selection schemes, namely, single-core state (SCS) and dual-core state (DCS) schemes since they correspond to a single and dual-core states[1], which adaptively select the NOMA or a buffer-aided cooperative mode according to the instantaneous buffer state and wireless environments. The core states are carefully chosen, which ensure not only a sufficient amount of available transmission modes or links but also a small number of stored packets at each buffer. In particular, the prioritization of the possible transmission modes for each buffer state is carefully designed, so that the SCS and DCS schemes enable the buffers likely to stay at the core states $(1,1)$ and $(1,0)$ (or $(0,1)$), respectively. The main contributions of this paper are summarized as follows:

- We propose two novel adaptive mode selection schemes for buffer-aided C-NOMA systems to achieve the favourable outage performance and the lowest delay, respectively.
- We derive the closed-form expressions for the system outage probability (SOP) and the average delay of the proposed schemes by analyzing the corresponding state transition probabilities.
- We perform asymptotic performance analysis in the high signal-to-noise ratio (SNR) regime, which reveals that both proposed schemes achieve the full diversity gain within the minimum required buffer size $L = 2$.

Now, we summarize the main differences between the proposed schemes and the P2N scheme in [34]. *Firstly*, different from the P2N scheme in [34] that always allocates the priority to the NOMA mode at any buffer state, the two proposed schemes allocate the priority to the NOMA mode only when the buffers are in several certain favourable states. *Secondly*, compared to the P2N scheme that prefers to stay at the buffer state of $(2,2)$, the proposed SCS and DCS schemes prefer to stay at the buffer states of $(1,1)$ and $(1,0)$ (or $(0,1)$), respectively, which are beneficial for the delay performance. *Thirdly*, to achieve the full diversity gain, the minimum required buffer sizes of the P2N scheme and either of the proposed schemes are $L = 3$ and $L = 2$, respectively. This implies that both proposed schemes significantly reduce the system delay and guarantees the outage performance simultaneously.

The structure of this paper is organized as follows. Section II describes the system model and the basic theories. In Section III, a framework for the outage-delay analysis of the proposed schemes is presented. The proposed SCS and DCS schemes are introduced and analyzed in Section IV and Section V, respectively. Section VI provides simulation results to show the performance of the proposed schemes. Finally, we conclude this paper in Section VII. The key notations used in this paper are defined in Table I. Moreover, throughout this paper, the SNR denotes the ratio of transmit power (not received power) to the noise variance, unless stated otherwise.

[1]In this paper, SCS refers to a buffer state whose stationary probability approaches 1 as the SNR is large; DCS refers to two buffer states, either of which has a stationary probability approaching 0.5 as the transmit SNR is large.

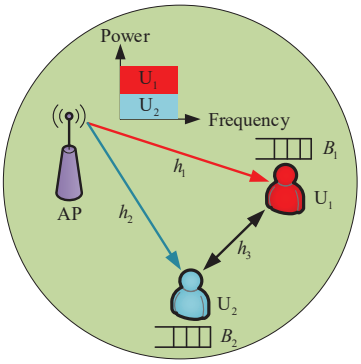

Fig. 1. System model of a buffer-aided C-NOMA system.

II. System Model and Preliminaries

In this section, we will briefly restate the system model and present some preliminaries regarding the development of the proposed schemes.

A. System Model

As shown in Fig. 1, consider a buffer-aided C-NOMA system, which consists of one AP and a pair of users (U_1 and U_2) sharing in the same frequency resource block. Each U_i is equipped with a buffer B_i, $i \in \{1,2\}$, and the two users perform bidirectional buffer-aided cooperation with each other. Each buffer B_i has $L \geq 2$ storage units, which is used to store a packet intended for the other user. Note that L denotes the buffer size, which represents the maximum number of packets each buffer can store instead of the actual stored number of packets in each time slot. Moreover, both buffers are empty during the initialization of the transmission process. It is assumed that the transmission period is divided into time slots of equal length, and each packet spans one time slot. In each time slot, the AP or one user is selected to transmit a packet. For the direct transmission, the AP uses NOMA to serve the users simultaneously directly. For the buffer-aided cooperative transmission, the AP first sends a mixed packet that includes both users' messages to the user, who has the strong link with the AP, and this user decodes the packet and stores the message of the other user in its buffer; then, each user forwards the packets stored in its buffer to the other user in certain time slots. In addition, the target data rate for U_i, $i \in \{1,2\}$, is predefined as R_i in bits per slot.

For the considered system model, independent and non-identical channel realizations are considered. Specifically, we denote h_i as the channel coefficient for the link AP $\rightarrow \mathrm{U}_i$, and denote h_3 as the common channel coefficient for the links U_1

TABLE I
LIST OF KEY NOTATIONS THROUGHOUT THE PAPER

Notation	Definition	Notation	Definition
L	Buffer size	$\vee$	or
U_i	User i	$\wedge$	and
B_i	Buffer i	α_i	Power allocation coefficient
R_i	Target data rate for U_i	P_b, ρ_b	Transmit power/SNR of the AP
h_i	Channel coefficient from the AP to U_i	P_u, ρ_u	Transmit power/SNR of the users
h_3	Channel coefficient between the users	l_i	The number of stored packets (buffer length) at buffer B_i
d_i	Distance between the AP and U_i	$\mathbf{A}$	State transition matrix
d_3	Distance between the two users	$\boldsymbol{\pi}$	Stationary state probability vector
γ	Path loss exponent	$\Pr\{\cdot\}$	Probability of an event
Ω_j	Mean of $\lvert h_j\rvert^2$	P_{out}	System outage probability
σ^2	Noise variance	$\overline{D}$	Average delay
$[x]^+$	$\max\{0, x\}$	$\bar{\mathcal{G}}$	Complementary set of $\mathcal{G}$
$\mathcal{M}_k$	Transmission mode k	$F_k^{(l_1,l_2)}$	Probability to select $\mathcal{M}_k$ at state (l_1, l_2)
$\mathcal{G}_k$	Required channel gain region for performing $\mathcal{M}_k$	$f(\rho)\doteq\rho^b$	Exponentially equality, i.e., $\lim_{\rho\to\infty}\frac{\log f(\rho)}{\log\rho}=b$
(l_1, l_2)	Buffer state	$f(\rho)\dot{\leq}\rho^b$	Exponentially inequality, i.e., $\lim_{\rho\to\infty}\frac{\log f(\rho)}{\log\rho}\leq b$

$\rightarrow \mathrm{U}_2$ and $\mathrm{U}_2 \rightarrow \mathrm{U}_1$. All channel links are assumed to be subject to frequency flat Rayleigh block fading, which remain constant during one time slot and change randomly from one time slot to another. Each channel coefficient is modeled as $h_j = d_j^{-\gamma/2} g_j$, where $j \in \{1, 2, 3\}$ and g_j follows a complex Gaussian distribution with a mean of zero and variance of one, i.e., $g_j \sim \mathcal{CN}(0, 1)$, γ is the path loss exponent and d_j denotes the corresponding distance. Specifically, d_1 and d_2 denote the distances between the AP and U_1 and U_2, respectively. d_3 denotes the distance between U_1 and U_2. In addition, the mean of $|h_j|^2$ is denoted by $\Omega_j = d_j^{-\gamma}$. All nodes are assumed to work in a half-duplex mode, and each user receives a complex Gaussian noise with mean zero and variance σ^2.

B. Transmission Modes

Because the NOMA and buffer-aided cooperative transmission modes between the users are considered, there are six possible transmission modes, namely, $\mathcal{M}_0, \mathcal{M}_1, ..., \mathcal{M}_5$. Specifically, $\mathcal{M}_k$ represents the NOMA mode if $k = 0$, a cooperative mode if $k \in \{1, 2, ..., 4\}$ and the silent mode if $k = 5$. The AP selects a transmission mode at the beginning of each time slot based on channel estimation and consistently monitoring each buffer length. Then, these possible transmission modes are described in detail as follows:

1) Mode $\mathcal{M}_0$: The AP directly sends a superposition signal to the two users by using the NOMA scheme. Hence, they can be performed $\forall l_i$, $i \in \{1, 2\}$, where l_i denotes the number of stored packets (buffer length) at buffer B_i, and $0 \leq l_i \leq L$, $i \in \{1, 2\}$.

2) Mode $\mathcal{M}_1$: The AP maps the two users' packets into one mixed packet by using the one-to-one mapping criterion [10], and then transmits it to U_1. Thus, mode $\mathcal{M}_1$ can be performed requires the corresponding buffers to be not full, i.e., $l_1 < L$.

3) Mode $\mathcal{M}_2$: The AP transmits the two users' mixed packets to U_2. Thus, mode $\mathcal{M}_2$ can be performed requires the corresponding buffers to be not full, i.e., $l_2 < L$. Note that, due to channel randomness, both modes $\mathcal{M}_1$ and $\mathcal{M}_2$ are necessary to perform the bidirectional buffer-aided user cooperation.

4) Mode $\mathcal{M}_3$: U_1 sends a packet stored in its buffer to U_2, so it requires the buffer B_1 not to be empty, i.e., $l_1 > 0$.

5) Mode $\mathcal{M}_4$: U_2 sends a packet stored in its buffer to U_1, so it requires the buffer B_2 not to be empty, i.e., $l_2 > 0$.

6) Mode $\mathcal{M}_5$: All nodes keep silent, i.e., they neither transmit nor receive any packets, whose required buffer requirement is arbitrary, i.e., $\forall l_1, l_2$.

Remark 1: The AP is assumed to oversee mode controlling. Compared to the buffer-aided cooperative system models in existing works (e.g., [18]-[34]), the considered system model does not require additional system overhead. Specifically, at the beginning of each time slot, each user transmits pilot symbols so that the AP obtains the CSI of h_1 and h_2; each user also feeds back a one-bit message to inform the AP whether h_3 lies in $\mathcal{G}_3$ or $\mathcal{G}_4$. Moreover, it is trivial for the cost to keep track of the buffer length of each user.

Remark 2: The considered system model can also be extended to scenarios with more than two users. Assume without generality that there exist K users, and K is an even number. In this scenario, it is appropriate to employ the user pairing technique, that is commonly used in NOMA systems (e.g., [27], [30], [36]), to reduce the system complexity. Specifically, the K users are equally divided into $K/2$ groups, where each group includes a pair of users and is allocated one OFDMA subcarrier. Moreover, these users are assumed to be paired according to their locations, so the two users in one group are close to each other to perform buffer-aided mutual user cooperation. The details of the optimal resource allocation for the user pairing are out of the scope of this paper, which could be an interesting future topic.

C. Related Definitions

For the sake of easy description, a series of related definitions are provided in this subsection.

1) Related Parameters: Several related parameters are defined as follows:

- Let P_b and P_u denote the power constraints at the AP and each user, respectively; accordingly, $\rho_b \triangleq P_b/\sigma^2$, $\rho_u \triangleq P_u/\sigma^2$ denote the transmit SNR at the AP and each user, respectively, where δ^2 is the noise power at each receiver.
- α_i denotes the power allocation (PA) factor for the user with the order i when performing NOMA in mode $\mathcal{M}_0$,

where $i = 1, 2$, and without loss of generality, we assume that $\alpha_1 > \alpha_2$ and $\alpha_1 + \alpha_2 = 1$.

- $\hat{\alpha}_i \triangleq \left[1 - 2^{R_i}\alpha_2\right]^+$, $\epsilon_{b1} \triangleq \left(2^{R_1} - 1\right)/\rho_b$, $\epsilon_{b2} \triangleq \left(2^{R_2} - 1\right)/\rho_b$, $\zeta_1 \triangleq \max\left\{\epsilon_{b1}/\hat{\alpha}_1, \epsilon_{b2}/\alpha_2\right\}$, and $\zeta_2 \triangleq \max\left\{\epsilon_{b2}/\hat{\alpha}_2, \epsilon_{b1}/\alpha_2\right\}$ are associated with the NOMA transmission (i.e., mode $\mathcal{M}_0$).
- $\xi_b \triangleq \left(2^{2(R_1+R_2)} - 1\right)/\rho_b$ is associated with the cooperative transmission from the AP to either U_1 or U_2 (i.e., mode $\mathcal{M}_1$ or $\mathcal{M}_2$).
- $\xi_{u2} \triangleq \left(2^{2R_2} - 1\right)/\rho_u$ and $\xi_{u1} \triangleq \left(2^{2R_1} - 1\right)/\rho_u$ are associated with the $\mathrm{U}_1 \to \mathrm{U}_2$ and $\mathrm{U}_2 \to \mathrm{U}_1$ transmissions (i.e., modes $\mathcal{M}_3$ and $\mathcal{M}_4$), respectively.

2) Required channel gain (CG) region: The required CG region for successfully performing the mode $\mathcal{M}_k$ is denoted by $\mathcal{G}_k$, i.e., $\mathcal{M}_k$'s CG requirement, where $k \in \{0, 1, ..., 5\}$.

III. Outage-Delay Analysis Framework

This section provides a general framework for the outage-delay performance analysis of the adaptive mode selection schemes in the considered buffer-aided C-NOMA system. Our analysis is based on the formulation of a Markov chain and the derivation of its transition matrix to model the evolution of the buffer states.

A. State Transition Matrix

Let $s \triangleq (l_1, l_2)$ denote the buffer state, which represents the lengths for the queues of the two buffers. There are a total $(L+1)^2$ states, and they form a Markov chain. Denote s_n as the nth buffer state, $n \in \{1, \ldots, (L+1)^2\}$. Moreover, let $\mathbf{A}$ denote the corresponding $(L+1) \times (L+1)$ state transition matrix[2], in which the entry in the ith row and the jth column, denoted by $\mathbf{A}_{i,j}$, is the transition probability to move from state s_j at time t to s_i at time $t+1$, i.e.,

$$\mathbf{A}_{i,j} \triangleq \Pr\{s_j \to s_i\} = \Pr\{X(t+1) = s_i | X(t) = s_j\}, \quad (1)$$

where $X(t)$ denotes the random process of the instantaneous buffer state in each time slot. If the transition matrix $\mathbf{A}$ is column stochastic, irreducible and aperiodic[3], the stationary state probability vector can be obtained as follows [18]

$$\boldsymbol{\pi} = (\mathbf{A} - \mathbf{I} + \mathbf{B})^{-1}\mathbf{b}, \quad (2)$$

where $\boldsymbol{\pi} = [\pi_1, \pi_2, ..., \pi_{(L+1)^2}]^T$, $\mathbf{I}$ denotes the identity matrix, $\mathbf{b} = [1, 1, ..., 1]^T$ and $\mathbf{B}_{i,j} = 1$, $\forall i, j$.

B. SOP and Diversity

According to the transmission modes defined in Section II-B, we can observe that the target data rates for both users can be achieved, if either the NOMA mode or one buffer-aided cooperative mode can always be performed over a long period. However, there exists a probability that the silent mode $\mathcal{M}_5$ is selected, i.e., all the wireless channel links are so weak that neither the NOMA mode nor the buffer-aided cooperative modes can be performed. Therefore, an outage event in the proposed buffer-aided C-NOMA system is defined as the event that $\mathcal{M}_5$ is selected; namely, the AP and both users remain silent. By considering all possible buffer states, the SOP can be expressed as follows

$$P_{\mathrm{out}} = \sum_{n=1}^{(L+1)^2} \pi_n p_{\mathrm{out}}^{s_n} = \sum_{n=1}^{(L+1)^2} \pi_n F_5^{s_n}, \quad (3)$$

where $p_{\mathrm{out}}^{s_n}$ denotes the outage probability at state s_n, and we let $F_k^{s_n}$ denote the probability that the mode $\mathcal{M}_k$ is selected at state s_n, $k \in \{0, 1, ..., 5\}$.

Remark 3: In (3), we use $F_5^{s_n}$ rather than the commonly used $\mathbf{A}_{nn}$ (the probability that state s_n keeps unchanged) to express the outage probability at state s_n. This is because the buffer state remains unchanged when either the NOMA mode $\mathcal{M}_0$ or the silent mode $\mathcal{M}_5$ is selected, but an outage event occurs only when $\mathcal{M}_5$ is selected.

Based on the SOP and assuming that the transmit SNR for each node is $\rho_b = \rho_u = \rho$, the diversity gain of the C-NOMA system is defined as follows

$$d \triangleq -\lim_{\rho \to \infty} \frac{\log P_{\mathrm{out}}}{\log \rho}. \quad (4)$$

C. Average Delay

The system delay is formed by the delays at the AP and the users. Based on Little's law [38], the average delay at the AP can be expressed as $D_S = \frac{Q_S}{\eta_S}$, where Q_S and η_S denote the average sum queuing length and the sum transmit throughput at the AP, respectively. Similarly, the average delay at the users can be expressed as $D_U = \frac{Q_U}{\eta_U}$, where Q_U and η_U denote the average sum queuing length and the sum transmit throughput at the users, respectively. Then, the system average delay can be defined as

$$\overline{D} = D_S + r_c D_U, \quad (5)$$

in slots per packet, where r_c represents the percentage between the throughput associated with the cooperative modes and the total throughput. If the users have the same target rate $R_1 = R_2 = R_0$, we can obtain the closed-form expression of the average delay as

$$\overline{D} = \frac{1 + P_{\mathrm{out}} + \sum_{l_1=0}^{L}\sum_{l_2=0}^{L} \pi_{(l_1,l_2)} \left(2(l_1+l_2) - F_0^{(l_1,l_2)}\right)}{2(1 - P_{\mathrm{out}})}, \quad (6)$$

by following similar derivation steps with [34].

IV. Proposed SCS Scheme

In this section, a novel buffer state-based mode selection scheme is proposed, whose key feature is that only a SCS $(1, 1)$ exists. The main motivation to set $(1, 1)$ as the SCS is that it has the minimum sum buffer length among all buffer states that make all transmission modes available[4]. Therefore, keeping the buffer state at $(1, 1)$ is beneficial to achieve a low SOP and a low delay simultaneously.

[2] $\mathbf{A}$ varies according to different mode selection schemes, and the exact values of the elements in $\mathbf{A}$ will be derived later in the following sections.

[3] "Column stochastic": all entries in any column sum up to one; "irreducible": it is possible to move from any state to any state; "aperiodic": it is possible to return to the same state at any time [37].

[4] A transmission mode is said to be available if its buffer requirement shown in Section II-B is satisfied.

TABLE II
SCS SCHEME: PRIORITIZATION OF THE AVAILABLE MODES WITHIN DIFFERENT STATE REGIONS

State Class	State Region	Definition	Prioritization of the Available Modes
Class I	$\mathcal{L}_1^S$	$\{(l_1,l_2): 1 \le l_1 < l_2 < L\}$	$\mathcal{P}_0 > \mathcal{P}_4 > \mathcal{P}_3 > \mathcal{P}_1 > \mathcal{P}_2 > \mathcal{P}_5$
	$\mathcal{L}_2^S$	$\{(l_1,l_2): 1 \le l_2 < l_1 < L\}$	$\mathcal{P}_0 > \mathcal{P}_3 > \mathcal{P}_4 > \mathcal{P}_2 > \mathcal{P}_1 > \mathcal{P}_5$
	$\mathcal{L}_3^S$	$\{(l_1,l_2): 1 \le l_1 = l_2 < L\}$	$\mathcal{P}_0 > \mathcal{P}_3 = \mathcal{P}_4 > \mathcal{P}_1 = \mathcal{P}_2 > \mathcal{P}_5$
Class II	$\mathcal{L}_4^S$	$\{(l_1,l_2): l_1 = L, 1 \le l_2 < L\}$	$\mathcal{P}_3 > \mathcal{P}_0 > \mathcal{P}_4 > \mathcal{P}_2 > \mathcal{P}_5$
	$\mathcal{L}_5^S$	$\{(l_1,l_2): l_2 = L, 1 \le l_1 < L\}$	$\mathcal{P}_4 > \mathcal{P}_0 > \mathcal{P}_3 > \mathcal{P}_1 > \mathcal{P}_5$
	$\mathcal{L}_6^S$	$\{(l_1,l_2): l_1 = 0, 1 \le l_2 < L\}$	$\mathcal{P}_1 > \mathcal{P}_0 > \mathcal{P}_4 > \mathcal{P}_2 > \mathcal{P}_5$
	$\mathcal{L}_7^S$	$\{(l_1,l_2): l_2 = 0, 1 \le l_1 < L\}$	$\mathcal{P}_2 > \mathcal{P}_0 > \mathcal{P}_3 > \mathcal{P}_1 > \mathcal{P}_5$
Class III	$\mathcal{L}_8^S$	$\{(l_1,l_2): l_1 = L, l_2 = 0\}$	$\mathcal{P}_3 > \mathcal{P}_2 > \mathcal{P}_0 > \mathcal{P}_5$
	$\mathcal{L}_9^S$	$\{(l_1,l_2): l_2 = L, l_1 = 0\}$	$\mathcal{P}_4 > \mathcal{P}_1 > \mathcal{P}_0 > \mathcal{P}_5$
	$\mathcal{L}_{10}^S$	$\{(l_1,l_2): l_1 = l_2 = L\}$	$\mathcal{P}_3 = \mathcal{P}_4 > \mathcal{P}_0 > \mathcal{P}_5$
	$\mathcal{L}_{11}^S$	$\{(l_1,l_2): l_1 = l_2 = 0\}$	$\mathcal{P}_1 = \mathcal{P}_2 > \mathcal{P}_0 > \mathcal{P}_5$

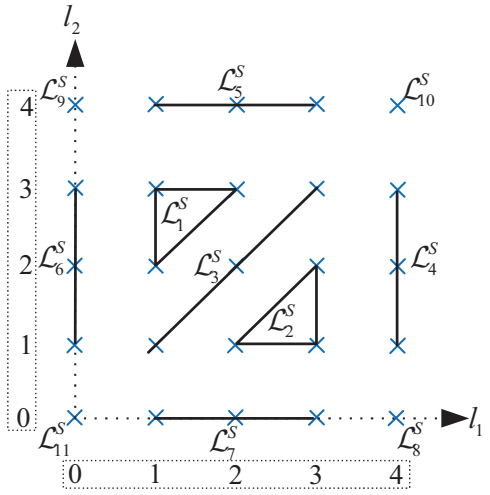

Fig. 2. Diagram of the considered state regions for the proposed SCS scheme, where $L = 4$, and the state regions $\mathcal{L}_1^S = \{(1,2),(1,3),(2,3)\}$, $\mathcal{L}_2^S = \{(2,1),(3,1),(3,2)\}$, $\mathcal{L}_3^S = \{(1,1),(2,2),(3,3)\}$, $\mathcal{L}_4^S = \{(4,1),(4,2),(4,3)\}$, $\mathcal{L}_5^S = \{(1,4),(2,4),(3,4)\}$, $\mathcal{L}_6^S = \{(0,1),(0,2),(0,3)\}$, $\mathcal{L}_7^S = \{(1,0),(2,0),(3,0)\}$, $\mathcal{L}_8^S = \{(4,0)\}$, $\mathcal{L}_9^S = \{(0,4)\}$, $\mathcal{L}_{10}^S = \{(4,4)\}$ and $\mathcal{L}_{11}^S = \{(0,0)\}$.

A. Proposed Scheme

As shown in Table II, we first divide the buffer states into eleven[5] different state regions. A diagram of the state regions with $L = 4$ is shown in Fig. 2. Second, define three different state classes to cluster these regions, where each class consists of the regions with similar properties. Then, the key step of the proposed SCS scheme is to design the prioritization of the available transmission modes within different state regions as shown in Table II, where $\mathcal{P}_k$ denotes the priority[6] of the mode $\mathcal{M}_k$, $k \in \{0,1,...,5\}$. Note that when $l_1 = l_2$, $\mathcal{P}_1 = \mathcal{P}_2$ (or $\mathcal{P}_3 = \mathcal{P}_4$), and we randomly select one from these two modes with equal probability. One mode will be selected during each time slot if its CG requirement can be satisfied but the other modes with higher priorities cannot. In the following, we will discuss the main idea behind the proposed SCS scheme in different classes.

1) Class I: Class I consists of the regions $\{\mathcal{L}_k^S\}_{k\in\{1,2,3\}}$, which represent the buffer states that both buffers are neither full nor empty. In this class, since all six modes are available, each buffer state is in an ideal condition from the SOP perspective, and the NOMA mode $\mathcal{M}_0$ occupies the highest priority, i.e., $\mathcal{M}_0$ will be selected as long as its CG requirement can be satisfied. The prioritization of the other modes is designed according to different state regions. For $\mathcal{L}_1^S$ with $l_2 > l_1$, buffer B_1 stores less packets than B_2, so we set $\mathcal{P}_4 > \mathcal{P}_3$ to preferentially decrease l_2 rather than l_1, and $\mathcal{P}_1 > \mathcal{P}_2$ to preferentially increase l_1 rather than l_2. Moreover, $\mathcal{M}_3$ has higher priority than $\mathcal{M}_1$ to reduce the delay at each buffer. Thus, the designed prioritization is $\mathcal{P}_0 > \mathcal{P}_4 > \mathcal{P}_3 > \mathcal{P}_1 > \mathcal{P}_2 > \mathcal{P}_5$. For $\mathcal{L}_2^S$ or $\mathcal{L}_3^S$, the prioritization is similarly designed.

2) Class II: Class II consists of the regions $\{\mathcal{L}_k^S\}_{k\in\{4,5,6,7\}}$, which represent the buffer states that one buffer is full or empty, but the other buffer is neither full nor empty. In this class, only five modes are available, and we give the highest priority to the full (empty) buffer to transmit (receive) a packet. For $\mathcal{L}_4^S$ with $l_1 = L$, $\mathcal{M}_3$ occupies the highest priority. Moreover, the priority of $\mathcal{M}_0$ is higher than $\mathcal{M}_4$ since buffer B_2 is in an ideal state; if the CG requirement of $\mathcal{M}_3$ is unsatisfied, we give priority to select $\mathcal{M}_0$ to perform a direct NOMA transmission without changing l_2. Then, $\mathcal{M}_4$ has a higher priority than $\mathcal{M}_2$ to reduce the delay at B_2. Thus, the designed prioritization for $\mathcal{L}_4^S$ is $\mathcal{P}_3 > \mathcal{P}_0 > \mathcal{P}_4 > \mathcal{P}_2 > \mathcal{P}_5$. For $\{\mathcal{L}_k^S\}_{k\in\{5,6,7\}}$, the prioritization is similarly designed.

3) Class III: Class III consists of the regions $\{\mathcal{L}_k^S\}_{k\in\{8,9,10,11\}}$, which represent the buffer states that each buffer is either full or empty. In this class, only four modes are available. In $\mathcal{L}_8^S$, we give the highest priority to the full buffer to transmit a packet, i.e., $\mathcal{M}_3$ occupies the highest priority. Moreover, $\mathcal{M}_2$ occupies the second-highest priority since the user with an empty buffer needs to receive data to make its buffer become not empty. If both $\mathcal{M}_3$ and $\mathcal{M}_2$ fail to perform, we will consider to select $\mathcal{M}_0$. Thus, the designed prioritization is $\mathcal{P}_3 > \mathcal{P}_2 > \mathcal{P}_0 > \mathcal{P}_5$, and the prioritization for $\mathcal{L}_9^S$ is similarly designed. For $\mathcal{L}_{10}^S$, $\mathcal{M}_3$ and $\mathcal{M}_4$ share the highest priority and the designed prioritization

[5]For $L = 2$, the state regions $\mathcal{L}_1^S$ and $\mathcal{L}_2^S$ become empty, and hence the number of non-empty state regions reduces to nine.

[6]In this paper, the priorities of the transmission modes are defined such that they are *determined* by the buffer state, which are independent of the instantaneous channel state. Therefore, the prioritization of the available modes can be predefined according to different buffer states. Based on the predefined prioritization, the adaptive mode selection process can be described as follows: we first consider the mode with the highest priority, which will be selected if its CG requirement is satisfied; otherwise, we consider the mode with the second highest priority, and so on.

is $\mathcal{P}_3 = \mathcal{P}_4 > \mathcal{P}_0 > \mathcal{P}_5$. A similar prioritization is designed for $\mathcal{L}_{11}^S$.

Remark 4: For the P2N scheme in [34], the NOMA mode always occupies the highest priority, which would impede to change a worse buffer state. However, the proposed SCS scheme gives the highest priority to the NOMA mode only in Class I where both buffers are neither full nor empty.

Remark 5: The conventional buffer state-based cooperative schemes in existing works (e.g., [34]) aim to keep each buffer to be neither full nor empty during most time slots. To this end, each buffer gives priority to receive a packet if its buffer length is smaller than the threshold of 2. However, for the proposed SCS scheme, each buffer gives priority to transmit rather than receive as long as it is not empty since each buffer can be kept in a SOP-ideal state by appropriately performing the NOMA mode.

B. Performance Analysis

To obtain the outage and delay performance of the proposed SCS scheme, the transition probabilities are given in the following proposition.

Proposition 1: The state transition matrix $\mathbf{A}$ of the Markov chain for the proposed SCS scheme is determined by the following transition probabilities.

- $P_{(l_1,l_2)}^{(l_1',l_2')}$, $P_{(l_1,l_2)}^{(l_1,l_2)}$, $P_{(l_1,l_2)}^{(l_1+1,l_2)}$ and $P_{(l_1,l_2)}^{(l_1-1,l_2)}$ are expressed in (8)-(11), respectively, as shown at the top of the next page, where, based on the definitions in II-C, several parameters are defined as follows:

$$\phi_0 \triangleq \exp\left(-\frac{\epsilon_{b1}}{\Omega_1\hat{\alpha}_1} - \frac{\zeta_1}{\Omega_2}\right) + \exp\left(-\frac{\zeta_2}{\Omega_1} - \frac{\epsilon_{b2}}{\Omega_2\hat{\alpha}_2}\right) - \exp\left(-\frac{\zeta_2}{\Omega_1} - \frac{\zeta_1}{\Omega_2}\right); \tag{7a}$$

$$\phi_1 \triangleq \exp\left(-\frac{\xi_b}{\Omega_1}\right)\left[1 - \exp\left(-\frac{\epsilon_{b2}}{\Omega_2\hat{\alpha}_2}\right)\right]; \tag{7b}$$

$$\phi_2 \triangleq \exp\left(-\frac{\xi_b}{\Omega_2}\right)\left[1 - \exp\left(-\frac{\epsilon_{b1}}{\Omega_1\hat{\alpha}_1}\right)\right]; \tag{7c}$$

$$\phi_3 \triangleq 1 - \phi_0 - \phi_1 - \phi_2; \tag{7d}$$

$$\varphi_i \triangleq \exp\left(-\frac{\xi_b}{\Omega_i}\right),\ i = 1, 2; \tag{7e}$$

$$\varphi_3 \triangleq \phi_0 - \exp\left(-\frac{\xi_b}{\Omega_1} - \frac{\epsilon_{b2}}{\Omega_2\hat{\alpha}_2}\right); \tag{7f}$$

$$\psi_0 \triangleq \exp\left(-\frac{\max\left(\xi_{u1}, \xi_{u2}\right)}{\Omega_3}\right); \tag{7g}$$

$$\psi_1 \triangleq \left[\exp\left(-\frac{\xi_{u2}}{\Omega_3}\right) - \exp\left(-\frac{\xi_{u1}}{\Omega_3}\right)\right]^+; \tag{7h}$$

$$\psi_2 \triangleq \left[\exp\left(-\frac{\xi_{u1}}{\Omega_3}\right) - \exp\left(-\frac{\xi_{u2}}{\Omega_3}\right)\right]^+; \tag{7i}$$

$$\psi_3 \triangleq 1 - \exp\left(-\frac{\min\left(\xi_{u1}, \xi_{u2}\right)}{\Omega_3}\right); \tag{7j}$$

  and in addition, $\mathcal{L}_{1-3}^S \triangleq \mathcal{L}_1^S \cup \mathcal{L}_2^S \cup \mathcal{L}_3^S$.
- $P_{(l_1,l_2)}^{(l_1,l_2+1)}$ and $P_{(l_1,l_2)}^{(l_1,l_2-1)}$ are identical to $P_{(l_1,l_2)}^{(l_1+1,l_2)}$ and $P_{(l_1,l_2)}^{(l_1-1,l_2)}$, after switching "1" and "2" in (10) and (11), respectively.

Proof: Please refer to Appendix A. ∎

In addition, the probability that $\mathcal{M}_5$ is selected at state (l_1, l_2) is expressed as follows

$$F_5^{(l_1,l_2)} = \begin{cases} \phi_3\psi_3, & \text{if } (l_1,l_2) \in \mathcal{L}_{1-3}^S \\ (1-\phi_0-\phi_2)\psi_3, & \text{if } (l_1,l_2) \in \mathcal{L}_4^S \\ (1-\phi_0-\phi_1)\psi_3, & \text{if } (l_1,l_2) \in \mathcal{L}_5^S \\ \phi_3(1-\psi_0-\psi_2), & \text{if } (l_1,l_2) \in \mathcal{L}_6^S \\ \phi_3(1-\psi_0-\psi_1), & \text{if } (l_1,l_2) \in \mathcal{L}_7^S \\ (1-\varphi_2-\varphi_4)(1-\psi_0-\psi_1), & \text{if } (l_1,l_2) \in \mathcal{L}_8^S \\ (1-\varphi_1-\varphi_3)(1-\psi_0-\psi_2), & \text{if } (l_1,l_2) \in \mathcal{L}_9^S \\ (1-\phi_0)\psi_3, & \text{if } (l_1,l_2) \in \mathcal{L}_{10}^S \\ \phi_3, & \text{if } (l_1,l_2) \in \mathcal{L}_{11}^S \\ 0, & \text{otherwise.} \end{cases} \tag{12}$$

The derivation steps of (12) are provided in Appendix A when deriving the value of $P_{(l_1,l_2)}^{(l_1,l_2)}$. Furthermore, the probability that $\mathcal{M}_0$ is selected at state (l_1, l_2) is expressed as

$$F_0^{(l_1,l_2)} = P_{(l_1,l_2)}^{(l_1,l_2)} - F_5^{(l_1,l_2)}. \tag{13}$$

By substituting (12) and Proposition 1 into (3), the SOP can be obtained. Then, by substituting (13) and Proposition 1 into (6), the average delay can be obtained.

C. High SNR Analysis

In particular, the system is assumed to begin in the state $(0,0) \in \mathcal{L}_{11}^S$. Therefore, during the first time slot, the mode $\mathcal{M}_1$ or $\mathcal{M}_2$ will be selected as shown in Table II, i.e., the system very likely moves to the state $(0,1) \in \mathcal{L}_6^S$ or $(1,0) \in \mathcal{L}_7^S$ in the high SNR regime. During the second time slot, the mode $\mathcal{M}_1$ or $\mathcal{M}_2$ will be selected, i.e., the system very likely moves to the state $(1,1) \in \mathcal{L}_3^S$. Then, the system very likely keeps unchanged at the SOP-ideal state $(1,1)$, since $\mathcal{M}_0$ will be selected with a very high probability. Therefore, the state $(1,1)$ occupies a stationary state probability that goes to one, i.e., $\pi_{(1,1)} \to 1$ as $\rho_b, \rho_u \to \infty$, which will also be verified via numerical results in Table IV.

By examining asymptotic behaviors of the outage and delay performance, we can obtain the following propositions.

Proposition 2: The full diversity gain of three can be achieved by the proposed SCS scheme, as long as $L \geq 2$.

Proof: Please refer to Appendix B. ∎

The conventional buffer state-based cooperative schemes in existing works (e.g., [19], [22], [27], [30], [34]) normally require $L \geq 3$ to achieve the full diversity for different cooperative systems. Proposition 2 unveils that the proposed SCS scheme further reduces the minimum requirement of L from 3 to 2 to achieve the full diversity for the considered C-NOMA system, which is beneficial to achieve a low delay without affecting the outage performance.

Proposition 3: For the proposed SCS scheme, when $\rho_b, \rho_u \to \infty$, the overall average delay of the buffer-aided C-NOMA system is $\overline{D} \to 2$.

Proof: As mentioned before, we know that $\pi_{(1,1)} \to 1$, $F_0^{(1,1)} \to 1$ and $P_{\text{out}} \to 0$ as $\rho_b, \rho_u \to \infty$. Recalling (6), we have $\overline{D} \to \frac{1+2(1+1)-1}{2} = 2$. ∎

$$P_{(l_1,l_2)}^{(l_1',l_2')}=0,\ \text{if}\ |l_1'-l_1|\geq 2\vee|l_2'-l_2|\geq 2\vee\{|l_1'=l_1\pm 1|\wedge|l_2'=l_2\pm 1|\}. \tag{8}$$

$$P_{(l_1,l_2)}^{(l_1,l_2)}=\begin{cases}\phi_3\psi_3+\phi_0, & \text{if } (l_1,l_2)\in\mathcal{L}_{1-3}^S\\ (1-\phi_0-\phi_2)\psi_3+\phi_0(1-\psi_0-\psi_1), & \text{if } (l_1,l_2)\in\mathcal{L}_4^S\\ (1-\phi_0-\phi_1)\psi_3+\phi_0(1-\psi_0-\psi_2), & \text{if } (l_1,l_2)\in\mathcal{L}_5^S\\ \phi_3(1-\psi_0-\psi_2)+\varphi_3, & \text{if } (l_1,l_2)\in\mathcal{L}_6^S\\ \phi_3(1-\psi_0-\psi_1)+\varphi_4, & \text{if } (l_1,l_2)\in\mathcal{L}_7^S\\ (1-\varphi_2)(1-\psi_0-\psi_1), & \text{if } (l_1,l_2)\in\mathcal{L}_8^S\\ (1-\varphi_1)(1-\psi_0-\psi_2), & \text{if } (l_1,l_2)\in\mathcal{L}_9^S\\ \psi_3, & \text{if } (l_1,l_2)\in\mathcal{L}_{10}^S\\ (1-\varphi_1)(1-\varphi_2), & \text{if } (l_1,l_2)\in\mathcal{L}_{11}^S\\ 0, & \text{otherwise.}\end{cases} \tag{9}$$

$$P_{(l_1,l_2)}^{(l_1+1,l_2)}=\begin{cases}\phi_1\psi_3, & \text{if } (l_1,l_2)\in\mathcal{L}_{1-3}^S\cup\mathcal{L}_5^S\\ \varphi_1, & \text{if } (l_1,l_2)\in\mathcal{L}_6^S\\ \phi_1(1-\psi_0-\psi_1), & \text{if } (l_1,l_2)\in\mathcal{L}_7^S\\ \varphi_1(1-\psi_0-\psi_2), & \text{if } (l_1,l_2)\in\mathcal{L}_9^S\\ \varphi_1[1-\frac{1}{2}\varphi_2], & \text{if } (l_1,l_2)\in\mathcal{L}_{11}^S\\ 0, & \text{otherwise.}\end{cases} \tag{10}$$

$$P_{(l_1,l_2)}^{(l_1-1,l_2)}=\begin{cases}(1-\phi_0)\psi_1, & \text{if } (l_1,l_2)\in\mathcal{L}_1^S\\ (1-\phi_0)(\psi_1+\psi_0), & \text{if } (l_1,l_2)\in\mathcal{L}_2^S\\ (1-\phi_0)[\psi_1+\frac{1}{2}\psi_0], & \text{if } (l_1,l_2)\in\mathcal{L}_3^S\cup\mathcal{L}_5^S\\ \psi_1+\psi_0, & \text{if } (l_1,l_2)\in\mathcal{L}_4^S\cup\mathcal{L}_8^S\\ (1-\phi_0-\phi_2)(\psi_1+\psi_0), & \text{if } (l_1,l_2)\in\mathcal{L}_7^S\\ \psi_1+\frac{1}{2}\psi_0, & \text{if } (l_1,l_2)\in\mathcal{L}_{10}^S\\ 0, & \text{otherwise.}\end{cases} \tag{11}$$

V. Proposed DCS Scheme

The proposed SCS scheme prefers to keep each buffer staying at the state $(1,1)$, which is beneficial to keep all transmission modes available as shown in Section IV. In this case, the full diversity can be achieved since an outage event occurs only if all wireless links are so weak that none of the CG requirements of the available transmission modes can be satisfied.

However, in this section, we propose the DCS scheme with two core states $(1,0)$ and $(0,1)$. This scheme is motivated by the fact that only one of the two links $\mathrm{U}_1\to\mathrm{U}_2$ and $\mathrm{U}_2\to\mathrm{U}_1$ is required to be available[7] to guarantee the full diversity of three, since the two links $\mathrm{U}_1\to\mathrm{U}_2$ an $\mathrm{U}_2\to\mathrm{U}_1$ share the same channel coefficient h_3. For instance, the full diversity can be guaranteed at the state $(1,0)$ since the three links $\mathrm{AP}\to\mathrm{U}_1$, $\mathrm{AP}\to\mathrm{U}_2$ and $\mathrm{U}_1\to\mathrm{U}_2$ are available. Therefore, keeping the buffer state at $(1,0)$ or $(0,1)$ is beneficial to achieve a very low delay without affecting the diversity gain.

A. Proposed Scheme

As shown in Table III, the buffer states are first divided into eleven[8] different state regions. A diagram of the state regions with $L=4$ is shown in Fig. 3. Second, four different classes are defined to cluster similar regions. Then, the key step of the proposed DCS scheme is to design the prioritization of the available transmission modes within different state regions as shown in Table III. In the following, the main idea behind the proposed DCS scheme is explained in different classes.

1) Class I: Class I consists of the regions $\mathcal{L}_1^D$ and $\mathcal{L}_2^D$, which represent the buffer states that one buffer is empty, but the other one is neither full nor empty. In this class, only five modes are available, and each buffer state is in the desired condition so that the NOMA mode $\mathcal{M}_0$ occupies the highest priority. When $(l_1,l_2)\in\mathcal{L}_1^D$, if $\mathcal{M}_0$ fails to perform, $\mathcal{M}_4$ will be considered to transmit a packet from B_2 to reduce the delay. Moreover, $\mathcal{P}_1>\mathcal{P}_2$ since $l_1<l_2$. Thus, the designed prioritization is $\mathcal{P}_0>\mathcal{P}_4>\mathcal{P}_1>\mathcal{P}_2>\mathcal{P}_5$. The prioritization for $\mathcal{L}_2^D$ is similarly designed.

2) Class II: Class II consists of the regions $\{\mathcal{L}_k^D\}_{k\in\{3,4,5\}}$, which represent the buffer states that both buffers are neither full nor empty, i.e., all six modes are available. In this class, each buffer state is in an ideal condition from the outage perspective rather than the delay perspective. To reduce the delay, we give the priority to transmit packets from the buffers, i.e., $\mathcal{M}_3$ and $\mathcal{M}_4$ occupy the two highest priorities. In $\mathcal{L}_3^D$, since $l_1<l_2$, naturally we have $\mathcal{P}_4>\mathcal{P}_3$ and $\mathcal{P}_1>\mathcal{P}_2$. Moreover, $\mathcal{M}_0$ will be considered if both $\mathcal{M}_4$ and $\mathcal{M}_3$ fail to perform. Thus, we have $\mathcal{P}_4>\mathcal{P}_3>\mathcal{P}_0>\mathcal{P}_1>\mathcal{P}_2>\mathcal{P}_5$. For $\mathcal{L}_4^D$ or $\mathcal{L}_5^D$, the prioritization is similarly designed.

[7]The link $\mathrm{AP}\to\mathrm{U}_i$ is said to be available if B_i, $i\in\{1,2\}$, is not full, while the link $\mathrm{U}_1\to\mathrm{U}_2$ ($\mathrm{U}_2\to\mathrm{U}_1$) is said to be available if B_1 (B_2) is not empty.

[8]For $L=2$, the state regions $\mathcal{L}_3^D$ and $\mathcal{L}_4^D$ become empty, and hence the number of non-empty state regions reduces to nine.

This article has been accepted for publication in IEEE Transactions on Vehicular Technology. This is the author's version which has not been fully edited and content may change prior to final publication. Citation information: DOI 10.1109/TVT.2022.3205806

TABLE III
DCS SCHEME: PRIORITIZATION OF THE AVAILABLE MODES WITHIN DIFFERENT STATE REGIONS

State Class	State Region	Definition	Prioritization of the Available Modes
Class I	$\mathcal{L}_1^D$	$\{(l_1,l_2): l_1=0, 1\le l_2<L\}$	$\mathcal{P}_0>\mathcal{P}_4>\mathcal{P}_1>\mathcal{P}_2>\mathcal{P}_5$
	$\mathcal{L}_2^D$	$\{(l_1,l_2): l_2=0, 1\le l_1<L\}$	$\mathcal{P}_0>\mathcal{P}_3>\mathcal{P}_2>\mathcal{P}_1>\mathcal{P}_5$
Class II	$\mathcal{L}_3^D$	$\{(l_1,l_2): 1\le l_1<l_2<L\}$	$\mathcal{P}_4>\mathcal{P}_3>\mathcal{P}_0>\mathcal{P}_1>\mathcal{P}_2>\mathcal{P}_5$
	$\mathcal{L}_4^D$	$\{(l_1,l_2): 1\le l_2<l_1<L\}$	$\mathcal{P}_3>\mathcal{P}_4>\mathcal{P}_0>\mathcal{P}_2>\mathcal{P}_1>\mathcal{P}_5$
	$\mathcal{L}_5^D$	$\{(l_1,l_2): 1\le l_1=l_2<L\}$	$\mathcal{P}_3=\mathcal{P}_4>\mathcal{P}_0>\mathcal{P}_1=\mathcal{P}_2>\mathcal{P}_5$
Class III	$\mathcal{L}_6^D$	$\{(l_1,l_2): l_1=L, 1\le l_2<L\}$	$\mathcal{P}_3>\mathcal{P}_4>\mathcal{P}_0>\mathcal{P}_2>\mathcal{P}_5$
	$\mathcal{L}_7^D$	$\{(l_1,l_2): l_2=L, 1\le l_1<L\}$	$\mathcal{P}_4>\mathcal{P}_3>\mathcal{P}_0>\mathcal{P}_1>\mathcal{P}_5$
Class IV	$\mathcal{L}_8^D$	$\{(l_1,l_2): l_1=L, l_2=0\}$	$\mathcal{P}_3>\mathcal{P}_0>\mathcal{P}_2>\mathcal{P}_5$
	$\mathcal{L}_9^D$	$\{(l_1,l_2): l_2=L, l_1=0\}$	$\mathcal{P}_4>\mathcal{P}_0>\mathcal{P}_1>\mathcal{P}_5$
	$\mathcal{L}_{10}^D$	$\{(l_1,l_2): l_1=l_2=L\}$	$\mathcal{P}_3=\mathcal{P}_4>\mathcal{P}_0>\mathcal{P}_5$
	$\mathcal{L}_{11}^D$	$\{(l_1,l_2): l_1=l_2=0\}$	$\mathcal{P}_1=\mathcal{P}_2>\mathcal{P}_0>\mathcal{P}_5$

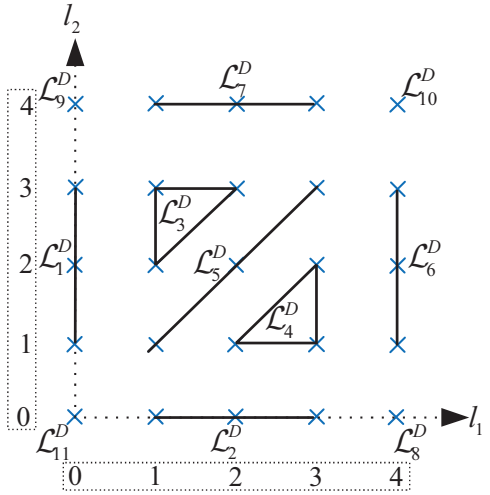

Fig. 3. Diagram of the considered state regions for the proposed DCS scheme, where $L=4$, and the state regions $\mathcal{L}_1^D=\{(0,1),(0,2),(0,3)\}$, $\mathcal{L}_2^D=\{(1,0),(2,0),(3,0)\}$, $\mathcal{L}_3^D=\{(1,2),(1,3),(2,3)\}$, $\mathcal{L}_4^D=\{(2,1),(3,1),(3,2)\}$, $\mathcal{L}_5^D=\{(1,1),(2,2),(3,3)\}$, $\mathcal{L}_6^D=\{(4,1),(4,2),(4,3)\}$, $\mathcal{L}_7^D=\{(1,4),(2,4),(3,4)\}$, $\mathcal{L}_8^D=\{(4,0)\}$, $\mathcal{L}_9^D=\{(0,4)\}$, $\mathcal{L}_{10}^D=\{(4,4)\}$ and $\mathcal{L}_{11}^D=\{(0,0)\}$.

3) Class III: Class III consists of the regions $\mathcal{L}_6^D$ and $\mathcal{L}_7^D$, which represent the buffer states that one buffer is full, but the other one is neither full nor empty. In this class, we give the highest priority to the full buffer to transmit a packet. Compared to $\mathcal{L}_3^D$ or $\mathcal{L}_4^D$ in Class II, only five modes are available; we only need to remove $\mathcal{P}_1$ ($\mathcal{P}_2$) from $\mathcal{L}_3^D$ ($\mathcal{L}_4^D$) when designing the prioritization for $\mathcal{L}_6^D$ ($\mathcal{L}_7^D$).

4) Class IV: Class IV consists of the regions $\{\mathcal{L}_k^D\}_{k\in\{8,9,10,11\}}$, which represent the buffer states that each buffer is either full or empty. In this class, only four modes are available, and the prioritization design is almost the same as Class III for the SCS scheme in Section IV. The only difference is to exchange $\mathcal{P}_2$ ($\mathcal{P}_1$) and $\mathcal{P}_0$ for $\mathcal{L}_8^D$ ($\mathcal{L}_9^D$), since allocating a lower priority to the mode $\mathcal{M}_2$ ($\mathcal{M}_1$) is beneficial to obtain a lower delay.

Remark 6: Unlike the proposed SCS scheme in Section IV that allocates the highest priority to the NOMA mode when both buffers are neither full nor empty, the proposed DCS scheme allocates the highest priority to the NOMA mode when one buffer is empty, but the other one is neither full nor empty, which aims to further reduce the delay.

B. Performance Analysis

The transition probabilities for the proposed DCS scheme are provided by the following proposition.

Proposition 4: The transition probabilities for the proposed DCS scheme are given as follows:

- $P_{(l_1,l_2)}^{(l_1',l_2')}$, $P_{(l_1,l_2)}^{(l_1,l_2)}$, $P_{(l_1,l_2)}^{(l_1+1,l_2)}$ and $P_{(l_1,l_2)}^{(l_1-1,l_2)}$ are expressed in (14)-(17), respectively, as shown at the top of the next page, where $\mathcal{L}_{3-5}^D \triangleq \mathcal{L}_3^D \cup \mathcal{L}_4^D \cup \mathcal{L}_5^D$;
- $P_{(l_1,l_2)}^{(l_1,l_2+1)}$ and $P_{(l_1,l_2)}^{(l_1,l_2-1)}$ are identical to $P_{(l_1,l_2)}^{(l_1+1,l_2)}$ and $P_{(l_1,l_2)}^{(l_1-1,l_2)}$, after switching "1" and "2" in (16) and (17), respectively.

Proof: By following similar derivation steps for Proposition 1 in Appendix A, this proposition can be proved, whose details are omitted for the sake of brevity. ■

In addition, similar to (12), the probability of selecting $\mathcal{M}_5$ at state (l_1,l_2) is expressed as follows

$$F_5^{(l_1,l_2)}=\begin{cases}\phi_3(1-\psi_0-\psi_2), & \text{if } (l_1,l_2)\in\mathcal{L}_1^D\\ \phi_3(1-\psi_0-\psi_1), & \text{if } (l_1,l_2)\in\mathcal{L}_2^D\\ \phi_3\psi_3, & \text{if } (l_1,l_2)\in\mathcal{L}_{3-5}^D\\ (1-\phi_0-\phi_2)\psi_3, & \text{if } (l_1,l_2)\in\mathcal{L}_6^D\\ (1-\phi_0-\phi_1)\psi_3, & \text{if } (l_1,l_2)\in\mathcal{L}_7^D\\ (1-\phi_0-\phi_2)(1-\psi_0-\psi_1), & \text{if } (l_1,l_2)\in\mathcal{L}_8^D\\ (1-\phi_0-\phi_1)(1-\psi_0-\psi_2), & \text{if } (l_1,l_2)\in\mathcal{L}_9^D\\ (1-\phi_0)\psi_3, & \text{if } (l_1,l_2)\in\mathcal{L}_{10}^D\\ \phi_3, & \text{if } (l_1,l_2)\in\mathcal{L}_{11}^D\\ 0, & \text{otherwise.}\end{cases} \tag{18}$$

By substituting (18) and Proposition 4 into (3), the SOP can be obtained. Furthermore, by substituting (18) and Proposition 4 into (6), the average delay can be obtained, using the relationship $F_0^{(l_1,l_2)}=P_{(l_1,l_2)}^{(l_1,l_2)}-F_5^{(l_1,l_2)}$.

C. High SNR Analysis

We assume that the system begins in the state $(0,0)\in\mathcal{L}_{11}^D$, and thus the mode $\mathcal{M}_1$ or $\mathcal{M}_2$ will be selected with a probability of almost 0.5 during the first time slot, as shown in Table III. Accordingly, there is a probability of almost 0.5 for the event that the buffer state moves to either $(0,1)\in\mathcal{L}_1^D$ or $(1,0)\in\mathcal{L}_2^D$ in the high SNR regime. After that, $\mathcal{M}_0$ will be selected with a very high probability and the system almost keeps unchanged at the state $(0,1)$ or $(0,1)$. Therefore, $(1,0)$ and $(0,1)$ occupy a stationary state probability that goes to

$$P_{(l_1,l_2)}^{(l_1',l_2')}=0,\ \text{if}\ |l_1'-l_1|\geq 2\vee|l_2'-l_2|\geq 2\vee\{|l_1'=l_1\pm 1|\wedge|l_2'=l_2\pm 1|\}. \tag{14}$$

$$P_{(l_1,l_2)}^{(l_1,l_2)}=\begin{cases}\phi_3(1-\psi_0-\psi_2)+\phi_0, & \text{if } (l_1,l_2)\in\mathcal{L}_1^D\\ \phi_3(1-\psi_0-\psi_1)+\phi_0, & \text{if } (l_1,l_2)\in\mathcal{L}_2^D\\ (1-\phi_1-\phi_2)\psi_3, & \text{if } (l_1,l_2)\in\mathcal{L}_{3-5}^D\\ (1-\phi_2)\psi_3, & \text{if } (l_1,l_2)\in\mathcal{L}_6^D\\ (1-\phi_1)\psi_3, & \text{if } (l_1,l_2)\in\mathcal{L}_7^D\\ (1-\phi_2)(1-\psi_0-\psi_1), & \text{if } (l_1,l_2)\in\mathcal{L}_8^D\\ (1-\phi_1)(1-\psi_0-\psi_2), & \text{if } (l_1,l_2)\in\mathcal{L}_9^D\\ \psi_3, & \text{if } (l_1,l_2)\in\mathcal{L}_{10}^D\\ (1-\varphi_1)(1-\varphi_2), & \text{if } (l_1,l_2)\in\mathcal{L}_{11}^D\\ 0, & \text{otherwise.}\end{cases} \tag{15}$$

$$P_{(l_1,l_2)}^{(l_1+1,l_2)}=\begin{cases}\phi_1(1-\psi_0-\psi_2), & \text{if } (l_1,l_2)\in\mathcal{L}_1^D\\ \phi_1(1-\psi_0-\psi_1), & \text{if } (l_1,l_2)\in\mathcal{L}_2^D\\ \phi_1\psi_3, & \text{if } (l_1,l_2)\in\mathcal{L}_{3-5}^D\cup\mathcal{L}_7^D\\ \phi_1(1-\psi_0-\psi_2), & \text{if } (l_1,l_2)\in\mathcal{L}_9^D\\ \varphi_1[1-\frac{1}{2}\varphi_2], & \text{if } (l_1,l_2)\in\mathcal{L}_{11}^D\\ 0, & \text{otherwise.}\end{cases} \tag{16}$$

$$P_{(l_1,l_2)}^{(l_1-1,l_2)}=\begin{cases}(1-\phi_0)(\psi_1+\psi_0), & \text{if } (l_1,l_2)\in\mathcal{L}_2^D\\ \psi_1, & \text{if } (l_1,l_2)\in\mathcal{L}_3^D\cup\mathcal{L}_7^D\\ \psi_1+\psi_0, & \text{if } (l_1,l_2)\in\mathcal{L}_4^D\cup\mathcal{L}_6^D\cup\mathcal{L}_8^D\\ \psi_1+\frac{1}{2}\psi_0, & \text{if } (l_1,l_2)\in\mathcal{L}_5^D\cup\mathcal{L}_{10}^D\\ 0, & \text{otherwise.}\end{cases} \tag{17}$$

TABLE IV
STATIONARY STATE PROBABILITIES FOR DIFFERENT SNRS, WHERE $L=2$ AND $R_1=R_2=0.5$ BITS/SLOT

Scheme	SNR (dB)	$\pi_{(0,0)}$	$\pi_{(0,1)}$	$\pi_{(0,2)}$	$\pi_{(1,0)}$	$\pi_{(1,1)}$	$\pi_{(1,2)}$	$\pi_{(2,0)}$	$\pi_{(2,1)}$	$\pi_{(2,2)}$
SCS	10	0.0428	0.0772	0.0006	0.1710	**0.6137**	0.0078	0.0155	0.0697	0.0017
	20	0.0005	0.0153	4E-06	0.0164	**0.9663**	0.0003	2E-05	0.0012	7E-07
	30	5E-06	0.0016	5E-09	0.0016	**0.9968**	3E-06	2E-08	1E-05	8E-11
DCS	10	0.1637	**0.1563**	0.0017	**0.5862**	0.0251	0.0005	0.0629	0.0035	0.0001
	20	0.0295	**0.4377**	0.0001	**0.5313**	0.0007	3E-07	0.0007	1E-06	7E-10
	30	0.0032	**0.4932**	2E-06	**0.5036**	8E-06	5E-11	6E-06	1E-10	1E-15

0.5, i.e., $\pi_{(0,1)},\pi_{(1,0)}\to\frac{1}{2}$ as $\rho_b,\rho_u\to\infty$, which will also be verified via numerical results in Table IV.

The following propositions present the diversity gain and average delay for the proposed DCS scheme.

Proposition 5: The proposed DCS scheme can also achieve the full diversity gain of three, $\forall L\geq 2$.

Proof: Please refer to Appendix C. ■

Proposition 6: For the proposed DCS scheme, when $\rho_b,\rho_u\to\infty$, the overall average delay of the buffer-aided C-NOMA system is $\overline{D}\to 1$.

Proof: As mentioned before, we know that $\pi_{(0,1)},\pi_{(1,0)}\to\frac{1}{2}$, $F_0^{(0,1)},F_0^{(1,0)}\to 1$ and $P_{\text{out}}\to 0$ as $\rho_b,\rho_u\to\infty$. Recalling (6), we have $\overline{D}\to\frac{1+\frac{1}{2}(2(1+0)-1)+\frac{1}{2}(2(0+1)-1)}{2}=1$. ■

Remark 7: Note that at least one stored packet at the buffers is necessary to make three links available and the full diversity achievable, which leads to an average system delay of at least 1 slot per packet. Therefore, Propositions 5 and 6 show that the proposed DCS scheme approaches the lowest delay in the high SNR regime among all schemes that can achieve the full diversity gain.

VI. NUMERICAL RESULTS

In this section, Monte Carlo simulations are employed for the buffer-aided C-NOMA system described in Section II, and several adaptive mode selection schemes are considered for performance comparison: the proposed SCS and DCS schemes in Section IV and Section V, respectively; the P2N scheme in [34]; the scheme with priority to transmit, which utilizes the basic idea behind the scheme in [21] so that each buffer prefers to transmit rather than receive as long as it is not empty; the selection bound is also used as a reference scheme, which refers to the SOP-optimal scheme where all buffer states are neither full nor empty in any time slot. The AP and the users are fixed at coordinates $(0,0)$ m, $(0,1)$ m and $(2,0)$ m, respectively, in a two-dimensional plane. For simplicity, both

This article has been accepted for publication in IEEE Transactions on Vehicular Technology. This is the author's version which has not been fully edited and content may change prior to final publication. Citation information: DOI 10.1109/TVT.2022.3205806

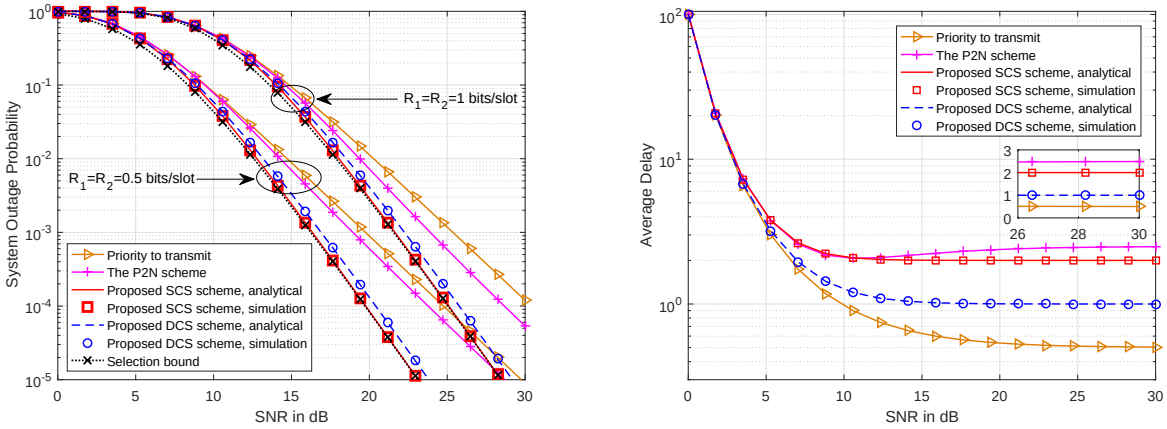

(a) SOP, where $R_1 = R_2 = 1$ or 0.5 bits/slot.

(b) Average delay, where $R_1 = R_2 = 0.5$ bits/slot.

Fig. 4. SOPs and average delays versus the transmit SNR in dB, where $\alpha_2 = 0.25$ and $L = 2$.

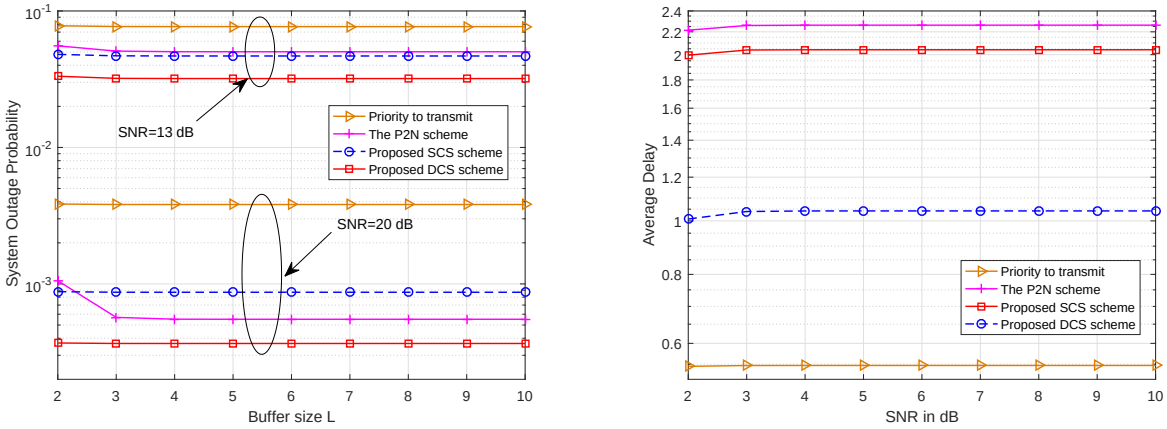

(a) SOP, where SNR= 13 or 20 dB.

(b) Average delay, where SNR= 20 dB.

Fig. 5. SOPs and average delays versus the buffer size L, where $\alpha_2 = 0.25$, $R_1 = 1$ bits/slot and $R_2 = 0.5$ bits/slot.

the AP and users are assumed to have the same transmit power and each user suffer the same receive noise power, so that both the AP and users have the same transmit SNR. We also set $\delta^2 = 1$, $\gamma = 2$ and $\alpha_2 = 0.25$, unless otherwise stated.

Remark 8: The proposed schemes and the comparative ones (i.e., the P2N scheme and the scheme with priority to transmit) have almost equal complexity in term of system overhead. First, all these schemes require full CSI at the AP, similar to most existing buffer-aided cooperative schemes that commonly require full CSI at a centralized node. Second, these schemes take mode priorities into consideration, so that all of them require the AP to know the buffer state by monitoring the identity of the selected transmission mode.

The numerical results in Table IV illustrate the stationary state probabilities of the two proposed schemes for $L = 2$, $R_1 = R_2 = 0.5$ bits/slot and SNR= 10, 20 and 30 dB. As shown by the numbers with frames in this table, the stationary probability of each core state for both proposed schemes gradually converges as the SNR increases. When SNR= 30 dB, $\pi_{(1,1)}$ approaches 1 for the SCS scheme; both $\pi_{(0,1)}$ and $\pi_{(1,0)}$ approach 0.5 for the DCS scheme. These observations verify the discussions in Sections IV-C and V-C.

Figs. 4(a) and 4(b) compare the SOP and the average delay performance of the proposed and comparative schemes versus the transmit SNR, respectively. We set $L = 2$ and $R_1 = R_2 = 1$ or 0.5 bits/slot. As shown in the two figures, the theoretical results match well with the simulation results. Fig. 4(a) shows that the two proposed schemes significantly outperform the P2N scheme in terms of the SOP, and the SCS scheme achieves the lowest SOP. The curves of the two proposed schemes have the same decreasing slope at high SNRs since both the two schemes achieve the full diversity when $L = 2$; whereas the SOP curve of the P2N scheme decreases more slowly at high SNRs since it cannot achieve the full diversity when $L = 2$. For example, if $R_1 = R_2 = 0.5$ bits/slot and the target SOP is 10^{-5}, the required SNR for the proposed SCS or DCS scheme is about 23 dB, whereas the required SNR of the P2N scheme is about 28 dB. Moreover, it is clearly shown that the outage performance of the SCS scheme achieves the selection bound when the SNR exceeds 15 dB because the SCS scheme likely keeps the buffers neither full nor empty in the high SNR regime as shown in Section

This article has been accepted for publication in IEEE Transactions on Vehicular Technology. This is the author's version which has not been fully edited and content may change prior to final publication. Citation information: DOI 10.1109/TVT.2022.3205806

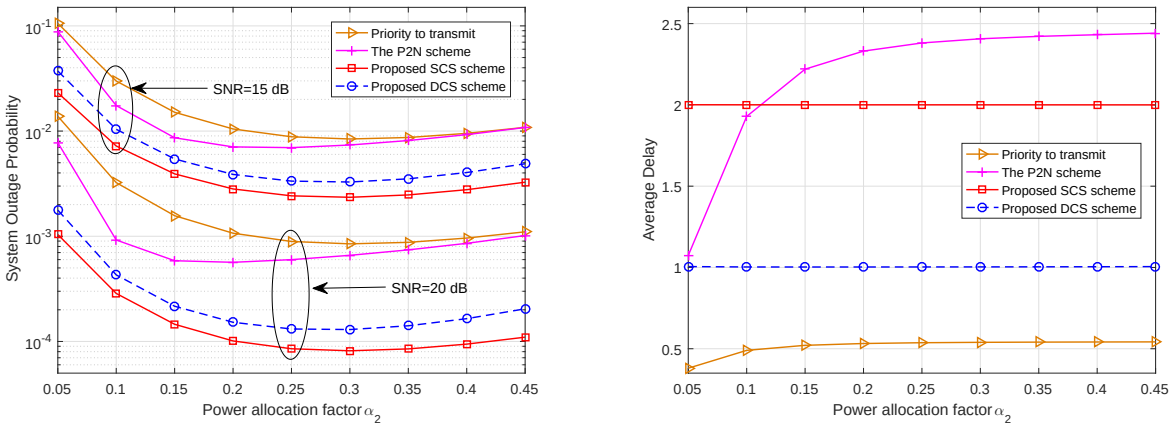

(a) SOP, where SNR= 15 or 20 dB.

(b) Average delay, where SNR= 20 dB.

Fig. 6. SOPs and average delays versus the PA factor α_2, where $L = 2$ and $R_1 = R_2 = 0.5$ bits/slot.

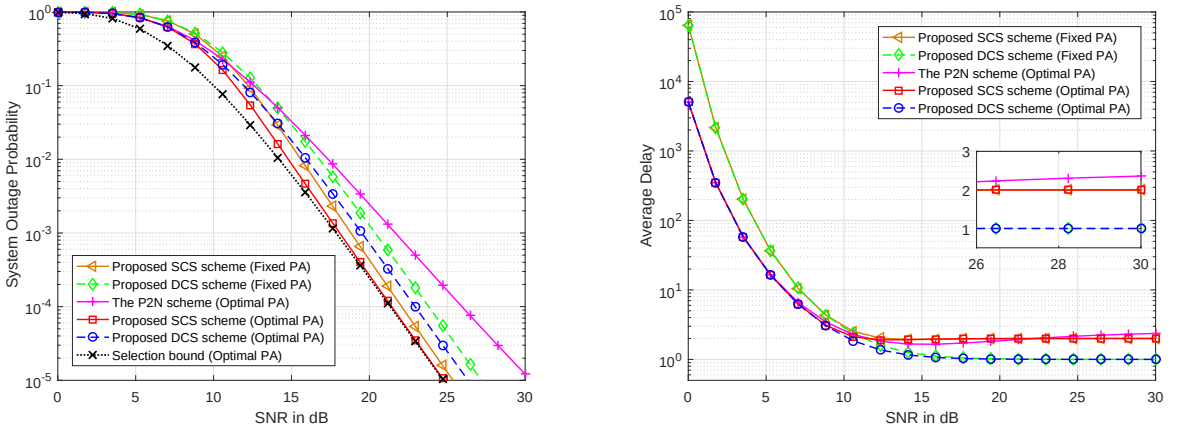

(a) SOP, where $R_1 = 0.5$ bits/slot, $R_2 = 1$ bits/slot.

(b) Average delay, where $R_1 = 0.5$ bits/slot, $R_2 = 1$ bits/slot.

Fig. 7. SOPs and average delays of several schemes with the fixed or optimal PA, where $\alpha_2 = 0.25$ and $L = 2$.

IV-C. Fig. 4(b) shows that the proposed SCS and DCS schemes achieve lower average delays than the P2N scheme when the SNR exceeds 2 and 11 dB, respectively. The average delays of the SCS and DCS schemes approach 2 and 1 slot per packet in the high SNR regime, consistent with Propositions 3 and 6, respectively. Moreover, the scheme with priority to transmit has the best delay performance but the worst outage performance.

Remark 9: One can observe from Fig. 4(b) that, for the P2N scheme, the average delay increases with the SNR when the SNR exceeds 10 dB. This observation can be explained as follows. Specifically, when the SNR is large enough, the CG requirement of each mode is likely to be satisfied, and each buffer likely stays at the length of 2 according to the mode selection policy in [34]. However, when the SNR becomes low or moderate, compared to $\mathcal{M}_3$ ($\mathcal{M}_4$), $\mathcal{M}_1$ ($\mathcal{M}_2$) is harder to be selected since its CG requirement is harder to be satisfied in the sense that both users' messages need to be transmitted. In this case, each buffer is prone to transmit rather than receive and each buffer length is likely to be 0 or 1, which ensures a lower average delay.

Figs. 5(a) and 5(b) show the SOP and the average delay performance versus the buffer size L, respectively, where we set $R_1 = 1$ bits/slot and $R_2 = 0.5$ bits/slot. The proposed SCS scheme not only outperforms the P2N and DCS schemes in terms of the SOP but also outperforms the P2N scheme in terms of the average delay. In Fig. 5(a), the DCS scheme outperforms the P2N scheme $\forall L \geq 2$ at a low SNR of 13 dB, but only for $L = 2$ at a high SNR of 20 dB. However, as shown in Fig. 5(b), the DCS scheme achieves the lowest average delay $\forall L \geq 2$, which is about a half of the average delay of the SCS or P2N scheme, since the system likely keeps at state $(0, 1)$ and $(1, 0)$ as shown in Section V-C. In addition, it is shown that the SOP and average delay for the proposed schemes decrease and increase with L, respectively, but the curves almost keep unchanged when $L \geq 3$. This is because the buffer states with small buffer lengths (i.e., 0, 1 or 2) are favored by the proposed and comparative schemes to reduce the system delay. Therefore, the proposed schemes are promising in the sense that they are appropriate to perform with only a small buffer size, which is beneficial to reduce the system delay without affecting the outage performance.

Figs. 6(a) and 6(b) present the comparison of SOPs and average delays as functions of the PA factor α_2, where we set $L = 2$ and $R_1 = R_2 = 0.5$ bits/slot. As shown in Fig. 6(a), both the proposed SCS and DCS schemes significantly outperform the P2N scheme in terms of the SOP. In addition, the SOP of each scheme first decreases and then increases with α_2 from 0.05 to 0.45. This is because the choice of a moderate PA factor α_2 is beneficial to balance the received SNRs of the two users and enhance the SOP when performing NOMA. Besides, it can be seen that the proposed schemes achieve the lowest SOP when α_2 is about 0.28. From Fig. 6(b), the average delay of the P2N scheme increases with α_2, whereas the average delays of the two proposed schemes almost keep unchanged as α_2 varies since the average delay is almost independent of α_2 at a high SNR of 20 dB, as shown in Propositions 3 and 6. Furthermore, it is clearly shown that the DCS scheme has the lowest average delay. For example, when $\alpha_2 = 0.15$, the DCS, SCS and P2N schemes achieve the average delays of about 1, 2 and 2.21 slots per packet, respectively.

Figs. 7(a) and 7(b) compare the SOP and the average delay performance of the proposed and comparative schemes versus the transmit SNR, respectively, by considering both the fixed and optimal PAs, where we set $L = 2$, $R_1 = 0.5$ bits/slot and $R_2 = 1$ bits/slot. For the optimal PA, the AP dynamically allocates the PA factors α_1 and α_2 based on the instantaneous CSI, to perform superposition coding for the NOMA mode, whose details can be found in [10], [27], [34]. From Fig. 7(a), one can observe that the optimal PA only brings a limited SOP performance improvement in comparison with the fixed PA, as the full diversity has been achieved by the proposed schemes with the fixed PA. It also should be noted that the optimal PA suffers a higher system overhead than the fixed PA, since the AP needs to inform both users the PA factors to perform decoding for the NOMA mode. Fig. 7(b) shows that, compared to the fixed PA, the optimal PA only benefits to the delay performance of the proposed schemes at a low SNR regime. However, when the SNR becomes large, the fixed and optimal PA schemes achieve almost the same average delay, since the asymptotic average delay of either the SCS or DCS scheme is independent of the PA factors as shown in Propositions 3 and 6.

VII. Conclusion

This paper investigated a buffer-aided C-NOMA system, where the NOMA and bidirectional buffer-aided cooperative transmission modes between the users are integrated. Two novel adaptive mode selection schemes (i.e., the SCS and DCS schemes) were proposed by designing the priorities of the NOMA and cooperative modes according to different buffer states. Then, the exact closed-form expressions of the SOP and the average delay of the proposed schemes were derived. We unveiled that the SCS and DCS schemes approached the lowest outage probability and the lowest average delay in certain scenarios, respectively. Finally, analytical and simulation results showed that both proposed schemes achieve the full diversity gain as long as $L \geq 2$, whereas conventional buffer-aided cooperative schemes require $L \geq 3$. A future direction of interest is to extend the proposed C-NOMA systems with hybrid buffer-aided cooperation, where the cooperation between intended users and the dedicated relay-based cooperation exists. Moreover, another future direction of interest is to adopt a distributed learning method to reduce the system overhead for channel acquisition.

Appendix A
Proof of Proposition 1

To prove Proposition 1, several related probabilities are first defined as follows.

- $\phi_0 = \Pr\{(|h_1|^2, |h_2|^2) \in \mathcal{G}_0\}$ denotes the probability of the required CG region $\mathcal{G}_0$ for the mode $\mathcal{M}_0$; $\phi_i = \Pr\{(|h_1|^2, |h_2|^2) \notin \mathcal{G}_0 \wedge |h_i|^2 \in \mathcal{G}_1\}$, $i = 1, 2$, denotes the probability that the CG requirement of $\mathcal{M}_0$ is unsatisfied but the CG requirement of $\mathcal{M}_i$ is satisfied.
- $\varphi_i = \Pr\{|h_i|^2 \in \mathcal{G}_i\}$, $i = 1, 2$, denotes the probability of the required CG region $\mathcal{G}_i$ for the mode $\mathcal{M}_i$; $\varphi_i = \Pr\{(|h_1|^2, |h_2|^2) \in \mathcal{G}_0 \wedge |h_1|^2 \notin \mathcal{G}_{i-2}\}$, $i = 3, 4$, denotes the probability that the CG requirement of $\mathcal{M}_0$ is satisfied but the CG requirement of $\mathcal{M}_{i-2}$ is unsatisfied.
- $\psi_0 = \Pr\{|h_3|^2 \in \mathcal{G}_3 \cap \mathcal{G}_4\}$ denotes the probability that both the CG requirements of the modes $\mathcal{M}_3$ and $\mathcal{M}_4$ are satisfied; $\psi_1 = \Pr\{|h_3|^2 \in \mathcal{G}_3 \cap \bar{\mathcal{G}}_4\}$ denotes the probability that the CG requirement of $\mathcal{M}_3$ is satisfied but the CG requirement $\mathcal{M}_4$ is unsatisfied; $\psi_2 = \Pr\{|h_3|^2 \in \bar{\mathcal{G}}_3 \cap \mathcal{G}_4\}$ is similarly defined; $\psi_3 = \Pr\{|h_3|^2 \in \bar{\mathcal{G}}_3 \cap \bar{\mathcal{G}}_4\}$ denotes the probability that neither CG requirements of these two modes are satisfied.

The mathematical expressions of these parameters have been given in (7), and more details can be found in our previous work in [34]. Now, based on these defined parameters and the proposed SCS scheme in Section IV, we can analyze different transition probabilities in the following, where we omit the superscript of $F_k^{(l_1,l_2)}$ (the probability that the mode $\mathcal{M}_k$ is selected) for simplicity.

1) In one time slot, since each buffer at most receives or transmits only one packet. Thus, $P_{(l_1,l_2)}^{(l_1',l_2')} = 0$ if $|l_i' - l_i| \geq 2$, where $i = 1, 2$, l_1' and l_2' represent two buffer lengths in the next slot, respectively. In addition, the two buffer lengths cannot change simultaneously according to the considered transmission modes. Thus, (8) can be easily obtained.
2) $P_{(l_1,l_2)}^{(l_1,l_2)}$ corresponds to the event that the mode $\mathcal{M}_0$ or $\mathcal{M}_5$ is selected, i.e., $P_{(l_1,l_2)}^{(l_1,l_2)} = F_0 + F_5$. According the designed prioritization for each state region shown in Table II, $P_{(l_1,L_2)}^{(l_1,L_2)}$ can be derived as follows:
   i) When $(l_1, l_2) \in \mathcal{L}_{1-3}^S$, $\mathcal{M}_0$ and $\mathcal{M}_5$ occupy the highest and lowest priorities, respectively. Thus, $F_0 = \phi_0$, and $F_5 = \phi_3\psi_3$ representing the probability that none of the CG requirements of $\{\mathcal{M}_k\}_{k\in\{0,1,\ldots,4\}}$ can be satisfied. Accordingly, $P_{(l_1,l_2)}^{(l_1,l_2)} = \phi_0 + \phi_3\psi_3$.
   ii) When $(l_1, l_2) \in \mathcal{L}_4^S$, the prioritization is $\mathcal{P}_3 > \mathcal{P}_0 > \mathcal{P}_4 > \mathcal{P}_2 > \mathcal{P}_5$; hence $\mathcal{M}_0$ will be selected if its CG requirement can be satisfied but $\mathcal{M}_3$'s CG requirement

cannot, i.e., $F_0 = \phi_0 \Pr\{|h_3|^2 \notin \mathcal{G}_3\} = \phi_0(1-\psi_0-\psi_1)$. Moreover, $F_5 = (1-\phi_0-\phi_2)\psi_3$ which denotes the probability that none of the CG requirements of $\{\mathcal{M}_k\}_{k\in\{0,2,3,4\}}$ can be satisfied. Similarly, $P_{(l_1,l_2)}^{(l_1,l_2)}$ can be obtained for $(l_1,l_2) \in \{\mathcal{L}_k^S\}_{k\in\{5,6,7\}}$.

iii) When $(l_1,l_2) \in \mathcal{L}_8^S$, the prioritization is $\mathcal{P}_3 > \mathcal{P}_2 > \mathcal{P}_0 > \mathcal{P}_5$; hence $\mathcal{M}_0$ will be selected if its CG requirement can be satisfied, but neither of the CG requirements of $\mathcal{M}_2$ and $\mathcal{M}_3$ can be satisfied, i.e., $F_0 = \varphi_4(1-\psi_0-\psi_1)$. Moreover, $F_5 = (1-\varphi_2-\varphi_4)(1-\psi_0-\psi_1)$ which denotes that probability that none of the CG requirements of $\{\mathcal{M}_k\}_{k\in\{0,2,3\}}$ can be satisfied. Similarly, $P_{(l_1,l_2)}^{(l_1,l_2)}$ can be obtained for $(l_1,l_2) \in \{\mathcal{L}_k^S\}_{k\in\{9,10,11\}}$.

3) $P_{(l_1,l_2)}^{(l_1+1,l_2)}$ corresponds to the event that the mode $\mathcal{M}_1$ is selected, and hence $P_{(l_1,l_2)}^{(l_1+1,l_2)} = F_1$. $\mathcal{M}_1$ is available only when $(l_1,l_2) \in \{\mathcal{L}_k^S\}_{k\in\{1,2,3,5,6,7,9,11\}}$. Here we only take $\mathcal{L}_1^S$ to illustrate the derivation of F_1. Specifically, when $(l_1,l_2) \in \mathcal{L}_1^S$, the prioritization is $\mathcal{P}_0 > \mathcal{P}_4 > \mathcal{P}_3 > \mathcal{P}_1 > \mathcal{P}_2 > \mathcal{P}_5$; hence $\mathcal{M}_1$ can be selected if its CG requirement can be satisfied, but none of the CG requirements of $\{\mathcal{M}_k\}_{k\in\{0,3,4\}}$ can be satisfied, and thus $F_1 = \phi_1\psi_3$. Moreover, one can verify that F_1 has the same value when $(l_1,l_2) \in \{\mathcal{L}_k^S\}_{k\in\{1,2,3,5\}}$, so we take the union set of these regions.

4) $P_{(l_1,l_2)}^{(l_1-1,l_2)}$ corresponds to the event that the mode $\mathcal{M}_3$ is selected, and hence $P_{(l_1,l_2)}^{(l_1-1,l_2)} = F_3$. $\mathcal{M}_3$ is available only when $(l_1,l_2) \in \{\mathcal{L}_k^S\}_{k\in\{1,2,3,4,5,7,8,10\}}$. Here we only take $\mathcal{L}_1^S$ to illustrate the derivation of F_3. Specifically, when $(l_1,l_2) \in \mathcal{L}_1^S$, $\mathcal{M}_3$ can be selected if its CG requirement can be satisfied, but neither of the CG requirements of $\mathcal{M}_0$ and $\mathcal{M}_4$ can be satisfied, and thus $F_3 = (1-\phi_0)\psi_1$. Moreover, one can verify that F_3 has the same value when $(l_1,l_2) \in \{\mathcal{L}_j^S\}_{k\in\{3,5\}}$ or $(l_1,l_2) \in \{\mathcal{L}_j^S\}_{k\in\{4,8\}}$.

In summary, the transition probabilities in (8)-(11) are obtained.

Appendix B
Proof of Proposition 2

To obtain the diversity of the proposed SCS scheme, without loss of generality, we focus on $L = 2$ since the outage probability at least does not increase with L. As shown in Fig. 8, there are $(2+1)^2 = 9$ buffer states. These states are divided into three sets, where $\hat{S}_1 \triangleq \{(1,1)\}$ represents the set of the SCS, while $\hat{S}_2 \triangleq \{(0,1),(1,0),(1,2),(2,1)\}$ and $\hat{S}_3 \triangleq \{(0,0),(0,2),(2,0),(2,2)\}$ represent the sets of the states that can transit to the SCS via one and two steps, respectively. These sets form a simplified Markov chain, where the transition probability from $\hat{S}_i$ in time t to $\hat{S}_j$ in time $t+1$ is defined as $\hat{P}_i^j \triangleq \Pr\{X(t+1) \in \hat{S}_j | X(t) \in \hat{S}_i\}$.

Now, exponential gains of the transition probabilities and stationary probabilities are derived. The exponential equality is defined in Table I, i.e., $f(\rho) \doteq \rho^b$ if $\lim_{\rho\to\infty} \frac{\log f(\rho)}{\log \rho} = b$, where b denotes the exponential gain of $f(\rho)$ [39]. To derive $\hat{P}_1^2$, we

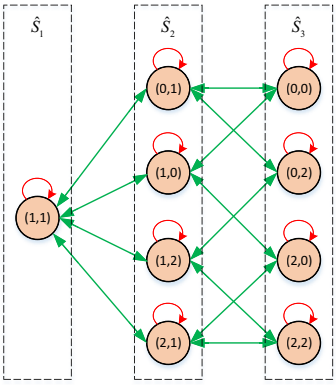

Fig. 8. Diagram of the formed state sets for the proposed SCS scheme, where $L = 2$.

first calculate the one-step transition probability $P_{(1,1)}^{(0,1)}$. From (11), as $\rho \to \infty$, $P_{(1,1)}^{(0,1)}$ can be expressed as follows

$$P_{(1,1)}^{(0,1)} = (1-\phi_0)\left(\psi_1 + \frac{1}{2}\psi_0\right) \approx (1-\phi_0) \doteq \rho^{-1}. \quad (19)$$

Similarly, $P_{(1,1)}^{(1,0)} \doteq \rho^{-1}$, $P_{(1,1)}^{(1,2)} \doteq \rho^{-2}$, and $P_{(1,1)}^{(2,1)} \doteq \rho^{-2}$ can be obtained, and thus

$$\begin{aligned}\hat{P}_1^2 &= \Pr\left\{X(t+1) \in \hat{S}_2 | X(t) \in \hat{S}_1\right\} \\ &= \sum_{s\in\hat{S}_1} \Pr\left\{X(t+1) \in \hat{S}_2 | X(t) = s\right\} \\ &\quad \times \Pr\left\{X(t) = s | X(t) \in \hat{S}_1\right\} \\ &= \sum_{i=1}^{4} P_{u_1}^{v_i} \Pr\left\{X(t) = u_1 | X(t) \in \hat{S}_1\right\} \\ &= \sum_{i=1}^{4} P_{u_1}^{v_i} \doteq \rho^{-1}, \end{aligned} \quad (20)$$

where we denote $u_1 = (1,1)$, $v_1 = (0,1)$, $v_2 = (1,0)$, $v_3 = (1,2)$ and $v_4 = (2,1)$.

Following similar derivation steps for $\hat{P}_1^2$, we have

$$\hat{P}_2^1 \doteq \rho^0, \ \hat{P}_2^3 \doteq \rho^{-1}, \ \hat{P}_3^2 \doteq \rho^0. \quad (21)$$

Based on (20), (21) and the fact that $\hat{P}_1^3 = \hat{P}_3^1 = 0$, the stationary probabilities of $\hat{S}_i$, denoted by $\hat{\pi}_i$, $i \in \{1,2,3\}$, can be expressed as follows

$$\hat{\pi}_1 \doteq \rho^0, \ \hat{\pi}_2 \doteq \rho^{-1}, \ \hat{\pi}_3 \doteq \rho^{-2}. \quad (22)$$

From (12), when $\rho \to \infty$, $F_5^{(1,1)}$ can be expressed as

$$F_5^{(1,1)} = \phi_3\psi_3 \doteq \rho^{-3}. \quad (23)$$

Similarly, we obtain

$$F_5^s \doteq \rho^{-2}, \ \forall s \in \hat{S}_i, \forall i \in \{2,3\}. \quad (24)$$

By substituting (22)-(24) into (3), the SOP of the proposed SCS scheme can be expressed as follows

$$P_{\text{out}} = \sum_{i=1}^{3} \sum_{s\in\hat{S}_i} F_5^s \hat{\pi}_i \doteq \rho^{-3}\rho^0 + \rho^{-2}\rho^{-1} + \rho^{-2}\rho^{-2} \doteq \rho^{-3}. \quad (25)$$

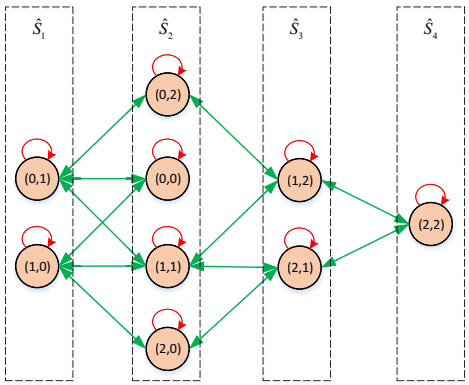

Fig. 9. Diagram of the constructed state sets for the proposed DCS scheme, where $L = 2$.

From (4), the diversity gain of three can be achieved by the proposed SCS scheme $\forall L \geq 2$.

Appendix C
Proof of Proposition 5

The diversity of the proposed DCS scheme can be obtained by following similar derivation steps with Appendix B. We also consider $L = 2$. However, the nine buffer states are divided into four state sets as shown in Fig. 9, where $\hat{S}_1 \triangleq \{(0,1),(1,0)\}$ represents the set of the DCSs, while $\hat{S}_2 \triangleq \{(0,0),(0,2),(2,0),(1,1)\}$, $\hat{S}_3 \triangleq \{(1,2),(2,1)\}$ and $\hat{S}_4 \triangleq \{(2,2)\}$ represent the sets of the states that can transit to $\hat{S}_1$ via one, two and three steps, respectively. From (16), when $\rho \to \infty$, $P_{(0,1)}^{(1,1)}$ can be approximated as

$$P_{(0,1)}^{(1,1)} = \phi_1(1-\psi_0-\psi_2) \doteq \rho^{-2}. \tag{26}$$

Moreover, $P_{(0,1)}^{(0,0)} \doteq \rho^{-1}$, $P_{(0,1)}^{(0,2)} \doteq \rho^{-2}$, $P_{(1,0)}^{(1,1)} \doteq \rho^{-2}$, $P_{(1,0)}^{(0,0)} \doteq \rho^{-1}$ and $P_{(1,0)}^{(2,0)} \doteq \rho^{-2}$ can be obtained. Thus, similar to (20), we have

$$\hat{P}_1^2, P_3^4 \doteq \rho^{-1},\ \hat{P}_2^3 \dot{\leq} \rho^{-1},\ \hat{P}_2^1, \hat{P}_3^2, \hat{P}_4^3 \doteq \rho^0, \tag{27}$$

where we use "$\dot{\leq}$" (defined in Table I) instead of "$\doteq$" for $\hat{P}_2^3$ since there exists a state $(0,0)$ in $\hat{S}_2$ that cannot transit to $\hat{S}_3$ via one step.

Since $\hat{P}_i^j = 0$ if $|i-j| \geq 2$, the stationary probabilities of $\hat{S}_i$ for the simplified Markov chain can be expressed as follows

$$\hat{\pi}_1 = \frac{\hat{P}_2^1\hat{P}_3^2\hat{P}_4^3}{\theta},\ \hat{\pi}_2 = \frac{\hat{P}_1^2\hat{P}_3^2\hat{P}_4^3}{\theta},$$
$$\hat{\pi}_3 = \frac{\hat{P}_1^2\hat{P}_2^3\hat{P}_4^3}{\theta},\ \hat{\pi}_4 = \frac{\hat{P}_1^2\hat{P}_2^3\hat{P}_3^4}{\theta}, \tag{28}$$

where $\theta \triangleq \hat{P}_2^1\hat{P}_3^2\hat{P}_4^3 + \hat{P}_1^2\hat{P}_3^2\hat{P}_4^3 + \hat{P}_1^2\hat{P}_2^3\hat{P}_4^3 + \hat{P}_1^2\hat{P}_2^3\hat{P}_3^4$.

Based on (27) and (28), we have

$$\hat{\pi}_i \dot{\leq} \rho^{-(i-1)},\ i \in \{1,2,3,4\}. \tag{29}$$

In addition, from (18), when $\rho \to \infty$, we have

$$F_5^{(0,1)} \doteq \rho^{-3},\ F_5^{(1,0)} \doteq \rho^{-3},\ F_5^s \doteq \rho^{-2},$$
$$\forall s \in \hat{S}_i, \forall i \in \{2,3,4\}. \tag{30}$$

By substituting (29) and (30) into (3), the SOP of the proposed DCS scheme can be exponentially bounded as follows

$$P_{\text{out}} = \sum_{i=1}^{4}\sum_{s\in\hat{S}_i} F_5^s\hat{\pi}_i$$
$$\dot{\leq} \rho^{-3}\rho^0 + \rho^{-2}\rho^{-1} + \rho^{-2}\rho^{-2} + \rho^{-2}\rho^{-3} \doteq \rho^{-3}. \tag{31}$$

From (4), the diversity gain of three can be achieved by the proposed DCS scheme $\forall L \geq 2$.

References

[1] Z. Ding, Z. Yang, P. Fan, and H. V. Poor, "On the performance of non-orthogonal multiple access in 5G systems with randomly deployed users," *IEEE Signal Process. Lett.*, vol. 21, no. 12, pp. 1501–1505, Dec. 2014.

[2] Z. Ding, Y. Liu, J. Choi, Q. Sun, M. Elkashlan, C. I, and H. V. Poor, "Application of non-orthogonal multiple access in LTE and 5G networks," *IEEE Commun. Mag.*, vol. 55, no. 2, pp. 185–191, Feb. 2017.

[3] Z. Ding, X. Lei, G. K. Karagiannidis, R. Schober, J. Yuan, and V. K. Bhargava, "A survey on non-orthogonal multiple access for 5G networks: Research challenges and future trends," *IEEE J. Sel. Areas in Commun.*, vol. 35, no. 10, pp. 2181–2195, Oct. 2017.

[4] Y. Liu, Z. Qin, M. Elkashlan, Z. Ding, A. Nallanathan, and L. Hanzo, "Non-orthogonal multiple access for 5G and beyond," *Proceedings of the IEEE*, vol. 105, no. 12, pp. 2347–2381, Oct. 2017.

[5] C. Huang, G. Chen, Y. Gong, P. Xu, Z. Han, and J. A. Chambers, "Buffer-aided relay selection for cooperative hybrid NOMA/OMA networks with asynchronous deep reinforcement learning," *IEEE J. Sel. Areas in Commun.*, vol. 39, no. 8, pp. 2514–2525, Jun. 2021.

[6] J. Kim and I. Lee, "Non-orthogonal multiple access in coordinated direct and relay transmission," *IEEE Commun. Lett.*, vol. 19, no. 11, pp. 2037–2040, Nov. 2015.

[7] J. Men and J. Ge, "Non-orthogonal multiple access for multiple-antenna relaying networks," *IEEE Commun. Lett.*, vol. 19, no. 10, pp. 1686–1689, Oct. 2015.

[8] M. F. Kader, M. B. Shahab, and S. Y. Shin, "Exploiting non-orthogonal multiple access in cooperative relay sharing," *IEEE Commun. Lett.*, vol. 21, no. 5, pp. 1159–1162, May 2017.

[9] Z. Yang, Z. Ding, Y. Wu, and P. Fan, "Novel relay selection strategies for cooperative NOMA," *IEEE Trans. Veh. Tech.*, vol. 66, no. 11, pp. 10 114–10 123, Nov. 2017.

[10] P. Xu, Z. Yang, Z. Ding, and Z. Zhang, "Optimal relay selection schemes for cooperative NOMA," *IEEE Trans. Veh. Tech.*, vol. 67, no. 8, pp. 7851–7855, Aug. 2018.

[11] H. Liu, Z. Ding, K. J. Kim, K. S. Kwak, and H. V. Poor, "Decode-and-forward relaying for cooperative NOMA systems with direct links," *IEEE Trans. Wireless Commun.*, vol. 17, no. 12, pp. 8077–8093, Dec. 2018.

[12] Z. Ding, M. Peng, and H. V. Poor, "Cooperative non-orthogonal multiple access in 5G systems," *IEEE Commun. Lett.*, vol. 19, no. 8, pp. 1462–1465, Aug. 2015.

[13] Y. Liu, Z. Ding, M. Elkashlan, and H. V. Poor, "Cooperative non-orthogonal multiple access with simultaneous wireless information and power transfer," *IEEE J. Sel. Areas in Commun.*, vol. 34, no. 4, pp. 938–953, Apr. 2016.

[14] Z. Zhang, Z. Ma, M. Xiao, Z. Ding, and P. Fan, "Full-duplex device-to-device-aided cooperative nonorthogonal multiple access," *IEEE Trans. Veh. Tech.*, vol. 66, no. 5, pp. 4467–4471, May 2016.

[15] K. Janghel and S. Prakriya, "Performance of adaptive OMA/cooperative-NOMA scheme with user selection," *IEEE Commun. Lett.*, vol. 22, no. 10, pp. 2092–2095, Oct. 2018.

[16] Q. Y. Liau and C. Y. Leow, "Successive user relaying in cooperative NOMA system," *IEEE Wireless Commun. Lett.*, vol. 8, no. 3, pp. 921–924, Jun. 2019.

[17] G. Li, D. Mishra, Y. Hu, Y. Huang, and H. Jiang, "Adaptive relay selection strategies for cooperative NOMA networks with user and relay cooperation," *IEEE Trans. Veh. Tech.*, vol. 69, no. 10, pp. 11 728–11 742, Aug. 2020.

[18] I. Krikidis, T. Charalambous, and J. S. Thompson, "Buffer-aided relay selection for cooperative diversity systems without delay constraints," *IEEE Trans. Wireless Commun.*, vol. 11, no. 5, pp. 1957–1967, May 2012.

[19] S. Luo and K. C. Teh, "Buffer state based relay selection for buffer-aided cooperative relaying systems," *IEEE Trans. Wireless Commun.*, vol. 14, no. 10, pp. 5430–5439, Oct. 2015.

[20] G. Chen, Z. Tian, Y. Gong, and J. A. Chambers, "Decode-and-forward buffer-aided relay selection in cognitive relay networks," *IEEE Trans. Veh. Tech.*, vol. 63, no. 9, pp. 4723–4728, Nov. 2014.

[21] Z. Tian, Y. Gong, G. Chen, and J. A. Chambers, "Buffer-aided relay selection with reduced packet delay in cooperative networks," *IEEE Trans. Veh. Tech.*, vol. 66, no. 3, pp. 2567–2575, Mar. 2017.

[22] P. Xu, Z. Ding, I. Krikidis, and X. Dai, "Achieving optimal diversity gain in buffer-aided relay networks with small buffer size," *IEEE Trans. Veh. Tech.*, vol. 65, no. 10, pp. 8788–8794, Oct. 2016.

[23] S.-L. Lin and K.-H. Liu, "Relay selection for cooperative relaying networks with small buffers," *IEEE Trans. Veh. Technol.*, vol. 65, no. 8, pp. 6562–6572, Aug. 2015.

[24] B. Manoj, R. K. Mallik, and M. R. Bhatnagar, "Performance analysis of buffer-aided priority-based max-link relay selection in DF cooperative networks," *IEEE Trans. Commun.*, vol. 66, no. 7, pp. 2826–2839, July 2018.

[25] S. Joshi, B. Manoj, and S. P. Dash, "Buffer-aided AF cooperative relaying network with NOMA transmission scheme," in *IEEE Intl. Conf. Adv. Netw. and Telecommun. Syst. (ANTS)*, Dec. 2020, pp. 1–6.

[26] S. El-Zahr and C. Abou-Rjeily, "Threshold based relay selection for buffer-aided cooperative relaying systems," *IEEE Trans. Wireless Commun.*, vol. 20, no. 9, pp. 6210–6223, Apr. 2021.

[27] Q. Zhang, Z. Liang, Q. Li, and J. Qin, "Buffer-aided non-orthogonal multiple access relaying systems in Rayleigh fading channels," *IEEE Trans. Commun.*, vol. 65, no. 1, pp. 95–106, Jan. 2017.

[28] S. Luo and K. C. Teh, "Adaptive transmission for cooperative NOMA system with buffer-aided relaying," *IEEE Commun. Lett.*, vol. 21, no. 4, pp. 937–940, Apr. 2017.

[29] J. Li, X. Lei, P. D. Diamantoulakis, F. Zhou, P. Sarigiannidis, and G. K. Karagiannidis, "Resource allocation in buffer-aided cooperative non-orthogonal multiple access systems," *IEEE Trans. Commun.*, vol. 68, no. 12, pp. 7429–7445, Dec. 2020.

[30] M. Alkhawatrah, Y. Gong, G. Chen, S. Lambotharan, and J. A. Chambers, "Buffer-aided relay selection for cooperative NOMA in the Internet of Things," *IEEE Internet of Things J.*, vol. 6, no. 3, pp. 5722–5731, Jun. 2019.

[31] N. Nomikos, T. Charalambous, D. Vouyioukas, G. K. Karagiannidis, and R. Wichman, "Hybrid NOMA/OMA with buffer-aided relay selection in cooperative networks," *IEEE J. Sel. Topics in Signal Process.*, vol. 13, no. 3, pp. 524–537, Jun. 2019.

[32] N. Nomikos, T. Charalambous, D. Vouyioukas, R. Wichman, and G. K. Karagiannidis, "Integrating broadcasting and NOMA in full-duplex buffer-aided opportunistic relay networks," *IEEE Trans. Veh. Tech.*, vol. 69, no. 8, pp. 9157–9162, Aug. 2020.

[33] J. Ren, X. Lei, and P. Takis Mathiopoulos, "Jointly adaptive distributed beamforming and resource allocation for buffer-aided multiple-relay NOMA networks," *IEEE Trans. Commun., doi: 10.1109/TCOMM.2021.3109271*, 2021.

[34] P. Xu, Y. Wang, G. Chen, G. Pan, and Z. Ding, "Design and evaluation of buffer-aided cooperative NOMA with direct transmission in IoT," *IEEE Internet of Things J.*, vol. 8, no. 10, pp. 8145–8158, 2021.

[35] Z. Ding, P. Fan, and H. V. Poor, "Impact of user pairing on 5G nonorthogonal multiple-access downlink transmissions," *IEEE Trans. Veh. Technol.*, vol. 65, no. 8, pp. 6010–6023, Aug. 2016.

[36] Y. Sun, D. W. K. Ng, Z. Ding, and R. Schober, "Optimal joint power and subcarrier allocation for full-duplex multicarrier non-orthogonal multiple access systems," *IEEE Trans. Commun.*, vol. 65, no. 3, pp. 1077–1091, Mar. 2017.

[37] J. R. Norris and J. R. Norris, *Markov chains*. Cambridge university press, 1997, no. 2.

[38] J. D. Little and S. C. Graves, "Little's law," in *Building intuition*. Springer, 2008, pp. 81–100.

[39] K. Azarian, H. El Gamal, and P. Schniter, "On the achievable diversity-multiplexing tradeoff in half-duplex cooperative channels," *IEEE Trans. Inf. Theory.*, vol. 51, no. 12, pp. 4152–4172, Dec. 2005.

Peng Xu (Member, IEEE) received the B.Eng. and the Ph.D. degrees in electronic and information engineering from the University of Science and Technology of China, Anhui, China, in 2009 and 2014, respectively. From June 2014 to July 2016, he was working as a postdoctoral researchers with the Department of Electronic Engineering and Information Science, University of Science and Technology of China, Hefei, China. He is currently an Associated Professor with the School of Communication and Information Engineering, Chongqing University of Posts and Telecommunications (CQUPT), Chongqing, China. His current research interests include cooperative communications, information-theoretic secrecy, NOMA techniques and reconfigurable intelligent surface. Dr. Peng Xu received IEEE WIRELESS COMMUNICATIONS LETTERS Exemplary Reviewer (2015 and 2021) and Excellent Paper of Chongqing Association for Science and Technology (2018).

Yunwu Wang (Student Member, IEEE) received the B.Sc. degree in Department of Optical Information Science and Technology from the College of Post and Telecommunication of Wuhan Institute of Technology, Wuhan, China, in 2018, and the M.Sc. degree in electronic and communication engineering at the School of Communication and Information Engineering, Chongqing University of Posts and Telecommunications (CQUPT), Chongqing, China, in 2021. He is currently pursuing the Ph.D. degree with the School of Information Science and Engineering, Southeast University, Nanjing, China. His research interests include C-RAN and machine learning.

Gaojie Chen (S'09 – M'12 – SM'18) received the B.Eng. and B.Ec. Degrees in electrical information engineering and international economics and trade from Northwest University, China, in 2006, and the M.Sc. (Hons.) and PhD degrees in electrical and electronic engineering from Loughborough University, Loughborough, U.K., in 2008 and 2012, respectively. After graduation, he took up academic and research positions at DT Mobile, Loughborough University, University of Surrey, University of Oxford and University of Leicester, U.K. He is currently an Assistant Professor with the Institute for Communication Systems, 5GIC & 6GIC, University of Surrey, U.K. His current research interests include information theory, wireless communications, satellite communications, cognitive radio, the Internet of Things, secrecy communications, and random geometric networks. He received the Exemplary Reviewer Awards of the IEEE WIRELESS COMMUNICATIONS LETTERS in 2018, the IEEE TRANSACTIONS ON COMMUNICATIONS in 2019 and the IEEE COMMUNICATIONS LETTERS in 2020 and 2021; and Exemplary Editor Awards of the IEEE COMMUNICATIONS LETTERS and IEEE WIRELESS COMMUNICATIONS LETTERS in 2021 and 2022, respectively. He serves as an Associate Editor for the IEEE COMMUNICATIONS LETTERS, IEEE WIRELESS COMMUNICATIONS LETTERS, IEEE JOURNAL ON SELECTED AREAS IN COMMUNICATIONS - MACHINE LEARNING IN COMMUNICATIONS AND NETWORKS and *Electronics Letters* (IET).

Ioannis Krikidis (Fellow, IEEE) received the Diploma degree in computer engineering from the Computer Engineering and Informatics Department (CEID), University of Patras, Greece, in 2000, and the M.Sc. and Ph.D. degrees in electrical engineering from the École Nationale Supérieurennnn des Télécommunications (ENST), Paris, France, in 2001 and 2005, respectively.

From 2006 to 2007, he worked as a Postdoctoral Researcher with the ENST. From 2007 to 2010, he was a Research Fellow with the School of Engineering and Electronics, The University of Edinburgh, Edinburgh, U.K. He also has held research positions at the Department of Electrical Engineering, University of Notre Dame; the Department of Electrical and Computer Engineering, University of Maryland; the Interdisciplinary Centre for Security, Reliability and Trust, University of Luxembourg; and the Department of Electrical and Electronic Engineering, Niigata University, Japan. He is currently an Associate Professor at the Department of Electrical and Computer Engineering, University of Cyprus, Nicosia, Cyprus. His current research interests include wireless communications, cooperative networks, 5G communication systems, wireless powered communications, and secrecy communications. He was a recipient of the Young Researcher Award from the Research Promotion Foundation, Cyprus, in 2013, and the IEEE ComSoc Best Young Professional Award in Academia, 2016. He serves as an Associate Editor for the IEEE TRANSACTIONS ON WIRELESS COMMUNICATIONS, IEEE TRANSACTIONS ON GREEN COMMUNICATIONS AND NETWORKING, and IEEE WIRELESS COMMUNICATIONS LETTERS. He has been recognized by the Web of Science as a Highly Cited Researcher for 2017, 2018, and 2019. He has received the prestigious ERC Consolidator Grant.

Kai-Kit Wong (Fellow, IEEE) received the B.Eng., M.Phil., and Ph.D. degrees in electrical and electronic engineering from The Hong Kong University of Science and Technology, Hong Kong, in 1996, 1998, and 2001, respectively. After graduation, he took up academic and research positions at The University of Hong Kong; Lucent Technologies; Bell-Labs, Holmdel; the Smart Antennas Research Group, Stanford University; and the University of Hull, U.K. He is currently the Chair of wireless communications with the Department of Electronic and Electrical Engineering, University College London, U.K. His current research interests include 5G and beyond mobile communications, including topics such as massive MIMO, full-duplex communications, millimeter-wave communications, edge caching and fog networking, physical layer security, wireless power transfer and mobile computing, V2X communications, and of course cognitive radios. His few other unconventional research topics that he has set his heart on, including for example, fluid antenna communications systems, and team optimization. He is a fellow of IET. He was a co-recipient of the 2013 IEEE SIGNAL PROCESSING LETTERS Best Paper Award and the 2000 IEEE VTS Japan Chapter Award at the IEEE Vehicular Technology Conference in Japan, in 2000, and a few other international best paper awards. He is also on the Editorial Board of several international journals. He has been serving as a Senior Editor for IEEE COMMUNICATIONS LETTERS since 2012 and IEEE WIRELESS COMMUNICATIONS LETTERS since 2016. He is also an Area Editor of IEEE TRANSACTIONS ON WIRELESS COMMUNICATIONS. He had also previously served as an Associate Editor for IEEE SIGNAL PROCESSING LETTERS from 2009 to 2012 and an Editor for IEEE TRANSACTIONS ON WIRELESS COMMUNICATIONS from 2005 to 2011. He was also a Guest Editor for the Special Issue on Virtual MIMO of the IEEE JOURNAL ON SELECTED AREAS IN COMMUNICATIONS in 2013. He is currently a Guest Editor for the Special Issue on Physical Layer Security for 5G of the IEEE JOURNAL ON SELECTED AREAS IN COMMUNICATIONS.